

# Owen-Shapley Policy Optimization (OSPO): A Principled RL Algorithm for Generative Search LLMs

Abhijnan Nath<sup>1,2</sup> Alireza Bagheri Garakani<sup>1</sup> Tianchen Zhou<sup>1</sup> Fan Yang<sup>1</sup> Nikhil Krishnaswamy<sup>2</sup>

## Abstract

Large language models are increasingly trained via reinforcement learning for personalized recommendation tasks, but standard methods like GRPO rely on sparse, sequence-level rewards that create a *credit assignment gap*—obscuring which tokens drive success. This gap is especially problematic when models must infer latent user intent from under-specified language without ground truth labels, a reasoning pattern rarely seen during pretraining. We introduce OWEN-SHAPLEY POLICY OPTIMIZATION (OSPO), a framework that redistributes sequence-level advantages based on tokens’ *marginal* contributions to outcomes. Unlike value-model-based methods requiring additional computation, OSPO employs potential-based reward shaping via Shapley-Owen attributions to assign segment-level credit while preserving the optimal policy—directly from task feedback without parametric value models. By forming coalitions of semantically coherent units (phrases describing product attributes or sentences capturing preferences), OSPO identifies which response parts drive performance. Experiments on Amazon ESCI and H&M Fashion datasets show consistent gains over baselines, with notable test-time robustness to out-of-distribution retrievers unseen during training.

## 1. Introduction

Large language models (LLMs) are increasingly central to modern recommendation pipelines. They can synthesize nuanced user preference summaries, reformulate complex queries, and generate natural-language artifacts that condition downstream retrieval and ranking processes (Peng et al.,

<sup>1</sup>Amazon Science, Seattle, WA, USA <sup>2</sup>Department of Computer Science, Colorado State University, Fort Collins, CO, USA. <sup>†</sup> Work done during an internship at Amazon Science. Correspondence to: Abhijnan Nath <abhijnan.nath@colostate.edu>, Alireza Bagheri Garakani <alirezg@amazon.com>.

2025; Lin et al., 2025). A major factor driving this adoption is their ability to learn directly from explicit task feedback through Reinforcement Learning (RL), bypassing costly human annotations. This makes them especially effective in dynamic, personalized settings where fine-grained supervision is infeasible (Lin et al., 2025; Lightman et al., 2023; Cheng et al., 2025). Efficient algorithms such as Group-Relative Policy Optimization (GRPO) (Shao et al., 2024a) enable LLMs to optimize against verifiable sequence-level signals from black-box components—retrievers, rankers, or quality assessors—without requiring an external value model.

However, removing the value model introduces structural limitations in how feedback is represented and propagated during training. In single-turn generative recommendation systems<sup>1</sup>, two major issues emerge. First, without a value model to decompose feedback across the sequence, GRPO-style training assigns a single scalar advantage to the *entire* response, obscuring which phrases or reasoning segments actually drive downstream utility (Yue et al., 2025) and limiting interpretability and efficiency (Henderson et al., 2018; Shao et al., 2024a; Cao et al., 2025; Cheng et al., 2025). Second, the absence of a structured value function increases vulnerability to reward hacking, where the model overfits to surface-level cues in black-box retrievers or rankers that expose only scalar feedback rather than the internal semantics of task success (Stiennon et al., 2020; Skalse et al., 2025; Lin et al., 2025).

To address these limitations, we introduce **Owen-Shapley Policy Optimization** (OSPO), an attribution-based RL framework that redefines how gradients are distributed across generated tokens. Unlike standard policy gradients that treat all tokens uniformly (Williams, 1992b; Ahmadian et al., 2024; Shao et al., 2024b), OSPO asks: *which parts of the sequence truly earned the reward?* Leveraging Owen-Shapley values from cooperative game theory (Shapley, 1953; Owen, 1977; Winter, 1992; Ruess, 2024), it models semantically coherent token segments as players in a coalition game, estimating their true contribution to the observed reward.

<sup>1</sup>Single-turn contrasts with multi-turn search, where the LLM incrementally refines its reasoning through interactive context acquisition (Yao et al., 2022; Xi et al., 2025).

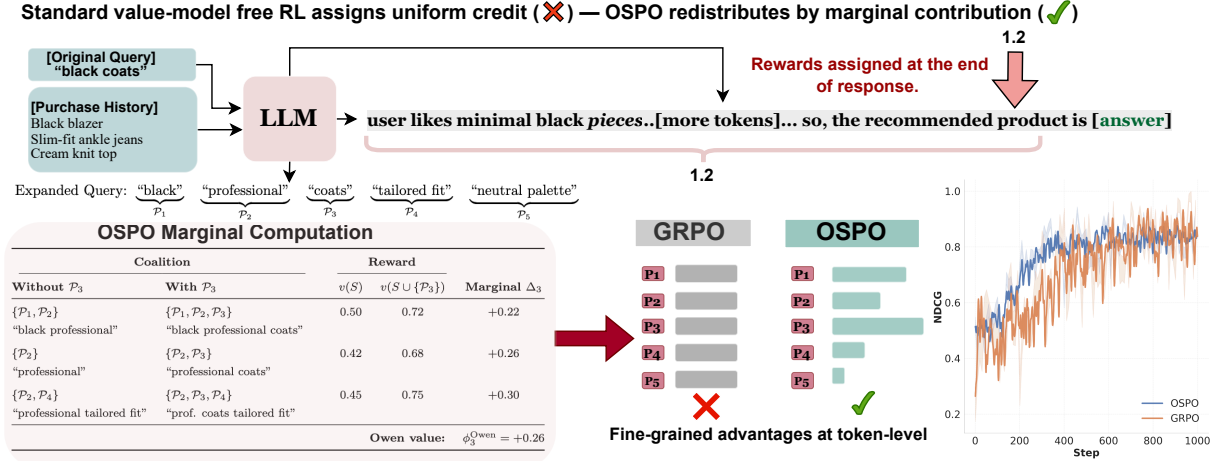


**Figure 1. OSPO overview: fine-grained credit assignment via Owen-Shapley values.** Standard value-model-free RL (e.g., GRPO (Shao et al., 2024a)) assigns uniform advantages (via a single terminal reward) to all tokens (grey bars), ignoring segment-level contributions. OSPO evaluates contiguous coalitions by querying a retriever (or a reward model) with partial sequences, computing each segment’s marginal contribution to retrieval quality. For example, the table shows coalition sampling for segment  $\mathcal{P}_3$  (“coats”): adding  $\mathcal{P}_3$  to coalition  $\{\mathcal{P}_1, \mathcal{P}_2\}$  increases the reward from 0.50 to 0.72, yielding marginal  $\Delta_3 = +0.22$ ; averaging such marginals across all coalitions produces the Owen value  $\phi_3^{\text{Owen}} = +0.26$ , indicating that “coats” consistently improves retrieval by providing explicit category information. These Owen values are then used to redistribute advantages proportionally to impact (center-right, teal bars) or “causally”, focusing gradient updates on truly high-contribution segments. Training dynamics (bottom-right) show OSPO reaches target performance in 50% fewer steps than GRPO, demonstrating improved sample efficiency.

For example, in product search, customers often make queries that contain attribute-specific preference signals expressed as phrases like “looking for [product] in **my usual neutral tones**” where the text in bold shows such a segment. OSPO treats these segments as high-level abstractions in the action space as valid segments for Owen-Shapley value computation, akin to options (Sutton, 1984) or macro-actions (Chai et al., 2025) in hierarchical RL. To assign such values, each segment’s marginal contribution to the total reward is measured by how much it increases the reward when added to different coalitions—segments that consistently improve outcomes receive credit, while those that dilute or distract are down-weighted. These attributions are obtained by querying any feedback model that returns scalar scores (e.g., a retriever or reward model), requiring no external value networks or process reward models (Schulman et al., 2017; Lightman et al., 2023).

Our key contribution is proposing a policy learning approach that can integrate such fine-grained value attributions from Owen values in learning good policies, while additionally leveraging from Monte-Carlo-based sampled rollouts that allow OSPO to achieve a reasonable trade off between exploration and exploitation (Sutton & Barto, 2018). **Our core insight in achieving this balance is one of gradient budget reallocation via advantage redistribution:** rather than spreading policy gradients uniformly across all tokens in a sequence (Shao et al., 2024a), OSPO concentrates updates on high-attribution segments while reducing signal on low-value content. Figure 1 illustrates OSPO’s advan-

tage redistribution mechanism that computes fine-grained advantages for the LLM’s response segments directly from task-based feedback or a reward model—weighted by the Owen attributions. Specifically, OSPO applies a simple mapping from segment-level Owen values to tokens that respects the scale of standard Monte-Carlo group-based advantages (Williams, 1992a), while reducing computation complexity involved in exact Shapley computations. This helps resolve the credit assignment gap inherent in learning *solely* from terminal rewards—*without compromising learning the final outcomes*. Additionally, in order to stabilize training dynamics, OSPO admits potential-based reward-shaping (PBRs) (Ng et al., 1999) to adapt segment-level Owen values to tokens—adopting the standard clip-surrogate objective for stable policy updates (Schulman et al., 2017). As Figure 1 demonstrates, this focused attribution yields substantially faster learning similar to prior work (Koo et al., 2025): OSPO reaches 85% NDCG in approximately 400 training steps on the fashion domain search task, while GRPO requires over 800 steps to approach similar performance despite identical training data and settings.

## 2. Related Work

**Generative Recommendation Systems.** LLMs have transformed recommendation systems through reasoning-driven decision-making (Wang et al., 2020; Zhao et al., 2018; Liu et al., 2023b). Recent methods integrate LLMs via feature enrichment (Xi et al., 2024; Li et al., 2023), rank-

ing (Geng et al., 2023; Luo et al., 2024), and conversational interaction (Zhou et al., 2020; Gao et al., 2023; Bang & Song, 2025). RL-LLM hybrids (Jeong et al., 2023; Sun et al., 2024; Lu et al., 2024; Rafailov et al., 2023b) enable personalization but focus on offline tuning. Building on RecR1 (Lin et al., 2025), which uses online task-specific feedback, OSPO addresses sparse credit assignment via Owen-Shapley attributions over segment-level spans. On the other hand, Owen-Shapley values have been explored across domains (Owen, 2014; Giménez Pradales & Puente del Campo, 2019; Lundberg & Lee, 2017) and applied in NLP for LLM interpretation (Goldshmidt & Horovitz, 2024; Mohammadi, 2024), prompt valuation (Liu et al., 2023a), model compression (Sun et al., 2025a), and dataset refinement (He et al., 2024). However, their use in RLHF remains limited. Recent work like SCAR (Cao et al., 2025) and Koo et al. (2025) extend Shapley-based reward distribution for LLM training.

**Densifying Sparse Rewards.** Dense feedback in policy optimization traditionally relies on value-function-based advantage estimation (Schulman et al., 2017; Kazemnejad et al., 2024; Yue et al., 2025; Azar et al., 2024; Pignatelli et al.), which is computationally heavy and requires learned critics. Value-model-free alternatives like GRPO and DPO (DeepSeek-AI et al., 2025; Rafailov et al., 2023b; Liu et al., 2025) reduce overhead but assign uniform credit or requires optimizing the discount factor in returns (Parthasarathi et al., 2025). Process Reward Models (Lightman et al., 2023; Wu et al., 2023; Bai et al., 2022; Choudhury, 2025) densify rewards via step-level supervision but require labeled intermediate steps and remain confined to deterministic domains (Fang et al., 2025; Sun et al., 2025b). Attention-based methods (Chan et al., 2024; Ng et al., 1999) propagate reward through attention weights but can entangle spurious correlations (Cao et al., 2025; Xie et al., 2025). Recent Shapley-based approaches like SCAR (Cao et al., 2025) compute principled marginal contributions but depend on parametric value models (Stiennon et al., 2020), restricting applicability to black-box feedback settings (Lin et al., 2025). In contrast, OSPO performs value-model-free advantage redistribution over segment-level Owen attributions, reducing Shapley’s exponential complexity while preserving fairness properties. Unlike SCAR, which redistributes rewards through a learned value model, OSPO directly redistributes advantages from policy rollouts, enabling end-to-end optimization without value computation.

### 3. Problem Formulation and Background

We model text generation for recommendation as a Markov Decision Process (MDP) defined by the tuple  $(\mathcal{S}, \mathcal{A}, P, r, \rho_0, \gamma)$ , where: the **state space**  $\mathcal{S}$  consists of all partial sequences  $(x, y_{<t})$  combining the input context  $x$  (e.g., user purchase history or raw search query) and to-

kens generated so far  $y_{<t} = (y_1, \dots, y_{t-1})$ ; the **action space**  $\mathcal{A}$  is the vocabulary from which the policy selects the next token  $y_t$ ; the **transition function**  $P(s_{t+1}|s_t, a_t)$  is deterministic—Appending token  $a_t = y_t$  to the history to form state  $s_{t+1} = (x, y_{<t})$ ; the **reward function**  $r : \mathcal{S} \times \mathcal{A} \rightarrow \mathbb{R}$  assigns scalar feedback; the **initial state distribution**  $\rho_0$  samples input  $x \sim \mathcal{D}$  from the data distribution; and the **discount factor**  $\gamma = 1$  for the undiscounted episodic setting as is standard for LLMs (Rafailov et al., 2024). A trajectory  $\tau = (s_0, a_0, s_1, a_1, \dots, s_T, a_T)$  corresponds to autoregressively generating a complete sequence  $y = (y_1, \dots, y_T)$  via the policy  $\pi_\theta(y_t|s_t) = \pi_\theta(y_t|x, y_{<t})$ , where  $\pi_\theta(y|x) = \prod_{t=1}^T \pi_\theta(y_t|x, y_{<t})$ .

The learning objective<sup>2</sup> is to find a policy that maximizes expected downstream performance:

$$\max_{\theta} \mathcal{J}(\theta) = \mathbb{E}_{x \sim \mathcal{D}, y \sim \pi_\theta(\cdot|x)} [r(x, y)], \quad (1)$$

where  $r(x, y) \in \mathbb{R}$  is a terminal reward from the downstream system—for instance, NDCG in product search or a reward-model score in user profile generation (Zheng et al., 2023).

Because  $r(x, y)$  is **sequence-level and terminal**, with  $r_t = 0$  for  $t < T$  and  $r_T = r(x, y)$ , the policy receives no signal about which tokens—or, more meaningfully, which *semantic segments* of the response—contributed to success, creating the credit assignment problem. To address sparse feedback, methods like **Group Relative Policy Optimization (GRPO)** (Shao et al., 2024a; Lin et al., 2025) replace the learned value function with a sampling-based baseline. GRPO samples  $G$  responses per prompt and computes group-relative advantages by normalizing rewards within the batch:

$$\hat{A}^{(g)} = \frac{r^{(g)} - \bar{r}}{\sigma_r}, \quad \text{where } \bar{r} = \frac{1}{G} \sum_{g'=1}^G r^{(g')}, \quad \sigma_r = \sqrt{\frac{1}{G} \sum_{g'=1}^G (r^{(g')} - \bar{r})^2}. \quad (2)$$

The GRPO objective is then:

$$\mathcal{J}^{\text{GRPO}}(\theta) = \frac{1}{G} \sum_{g=1}^G \frac{1}{T} \sum_{t=1}^T \min \left( \rho_t^{(g)} \hat{A}^{(g)}, \text{clip}(\rho_t^{(g)}, 1-\epsilon, 1+\epsilon) \hat{A}^{(g)} \right), \quad (3)$$

where  $\rho_t^{(g)} = \frac{\pi_\theta(y_t^{(g)}|x, y_{<t}^{(g)})}{\pi_{\theta_{\text{old}}}(y_t^{(g)}|x, y_{<t}^{(g)})}$  is the importance sampling ratio. While GRPO reduces variance via group normalization, it applies a *uniform advantage*  $\hat{A}^{(g)}$  to all tokens in a sequence (Samineni et al., 2025), offering no mechanism to distinguish which tokens—or meaningful semantic segments—actually drove the final reward  $r^{(g)}$ .

<sup>2</sup>We set the KL coefficient to  $\beta = 0$ , following prior work (Lin et al., 2025).

### 3.1. Owen-Shapley Policy Optimization: Segment-Level Credit Assignment

The mismatch between GRPO’s token-level uniform advantages and the compositional structure of recommendation tasks motivates a shift in granularity. To resolve this, our approach, OSPO, leverages the structure of Owen “coalitions” (Owen, 1977)—groups of segments or players in game theory—that compute what value *should* be assigned to each segment based on its *expected marginal contribution* to the total reward. Intuitively, this allows the policy  $\pi_\theta$  to learn which among the segments it generated actually led to the observed feedback. In other words, the policy learns counterfactually—reasoning over which parts of its response were relatively “more valuable” than others.

Specifically, let a generated response  $y^{(g)}$  from the policy  $\pi_\theta$  during group-based<sup>3</sup> sampling be decomposed into  $N$  semantically meaningful segments  $\mathcal{A}^{(g)} = \{a_1, \dots, a_N\}$ , where each  $a_j$  denotes a textual span corresponding to a linguistically coherent unit—such spans may represent noun phrases, adjective-noun pairs, or verb-led expressions or even full sentences depending on the task (see Section A.7 for extraction details). For any coalition  $S \subseteq \{1, \dots, N\}$ , we define the *characteristic function*  $v(S)$  as the reward obtained when only the segments indexed by  $S$  are present. To implement this, we construct a partial query  $y_S$  by concatenating the segments in coalition  $S$  while keeping the input context  $x$  fixed:  $y_S = a_i \oplus a_{i+1} \oplus \dots$  for  $i \in S$ , where  $\oplus$  denotes string concatenation.

Classical Shapley values (Shapley, 1953) assign to each segment  $j \in \{1, \dots, N\}$  its average marginal contribution across all possible subsets:

$$\phi_j = \sum_{S \subseteq \{1, \dots, N\} \setminus \{j\}} \frac{|S|!(N-|S|-1)!}{N!} (v(S \cup \{j\}) - v(S)). \quad (4)$$

This formulation ensures key fairness properties—*efficiency* ( $\sum_j \phi_j = v(\{1, \dots, N\})$ ), *symmetry*, and *linearity*—but quickly becomes intractable as  $N$  grows, requiring evaluation of  $2^N$  coalitions. The Owen value (Owen, 1977) extends Shapley’s framework by restricting the coalitions to a structured subset while preserving the core fairness guarantees (Owen, 2014). In our case, we impose a **contiguity constraint**: we only evaluate coalitions  $S = \{i, i+1, \dots, i+w-1\}$  consisting of consecutive segments, where  $w \leq w_{\max}$  is a maximum coalition width hyperparameter. This restriction serves two purposes: (1) it reduces computational complexity from  $O(2^N)$  to  $O(N \cdot w_{\max})$ , making online evaluation tractable during RL training, and (2) it preserves semantic coherence, as non-contiguous coalitions (e.g., skipping middle segments) would produce fragmented queries that may confound reward evaluation. We denote

<sup>3</sup>References to a response’s index in the group  $g$  are dropped when the context is clear.

the resulting segment attributions as  $\phi_j^{\text{Owen}}$ , computed by averaging marginal contributions  $v(S \cup \{j\}) - v(S)$  only over contiguous coalitions  $S$  where  $j \notin S$  but  $S \cup \{j\}$  remains contiguous:

$$\phi_j^{\text{Owen}} = \frac{1}{|C_j|} \sum_{S \in C_j} (v(S \cup \{j\}) - v(S)), \quad (5)$$

where  $C_j = \{S : S \text{ contiguous}, j \notin S, S \cup \{j\} \text{ contiguous}\}$  is the set of applicable coalitions for segment  $j$ . The full coalition generation and sampling strategy, including how we manage computational budgets via sampling when  $N$  is large, is detailed in Section A.6.

This coalitional view naturally aligns with the linguistic structure of LLM outputs in recommendation tasks, where contiguous spans—such as attribute–intent phrases (“blue midi dress”) or preference clauses (“prefers seasonal styles”)—form coherent compositional units. By assigning credit to these coalitions, OSPO captures how phrase combinations jointly influence downstream reward without enumerating all  $2^n$  subsets. Conceptually, this mirrors *options* or *temporal abstractions* in reinforcement learning (Sutton & Barto, 2018; Konidaris & Barto, 2009; Chai et al., 2025), allowing more efficient exploration and faster credit propagation across a response.

#### From Segment Attributions to Token Advantages.

While Owen values  $\phi_j^{\text{Owen}}$  quantify segment-level contributions, we must bridge two granularity gaps to effectively use such fine-grained values in policy optimization. First, standard baseline-based advantage computation requires exploring multiple completions per prompt via Monte Carlo sampling (Williams, 1992b; Kool et al., 2019) to estimate which responses are better than average—yielding per-sequence advantages  $\hat{A}^{(g)} = R^{(g)} - \bar{R}$  that indicate whether completion  $g$  should be reinforced or suppressed. Second, clipped surrogate objectives (Schulman et al., 2017; Yue et al., 2025; Shao et al., 2024a) operate at the “token” level, requiring decomposition of sequence-level feedback into token-level signals. Owen values address *within-sequence* attribution—identifying which segments contributed to quality—but the policy must also learn from these *between-sequence* group-level advantages to effectively explore and distinguish better completions from worse ones.

To achieve both objectives, our core insight is **advantage redistribution**: instead of uniform assignment, we redistribute the per-sequence advantages  $\hat{A}^{(g)}$  across tokens, weighted by their Owen values as computed above. This strategy allows us to leverage group-based advantages for variance reduction (Williams, 1992b; Kool et al., 2019) during exploration while learning fine-grained token attributions—overcoming the credit assignment problem without relying on an external value model. We construct a mapping  $W \in \mathbb{R}^{N \times T}$  where  $W_{it}$  encodes fraction of token span

covered by the segment  $a_i$  and token  $y_t$ , projecting segment Owen values to token space:  $\phi_{\text{tok}} = W^\top \phi_{\text{seg}}$ . After normalizing to unit sum  $\tilde{\phi}_t = \phi_t / \sum_{t'} \phi_{t'}$ , a naive proportional redistribution  $\tilde{A}_t = \hat{A}^{(g)} \cdot \tilde{\phi}_t$  would create severe length bias [Liu et al. \(2025\)](#); [Yue et al. \(2025\)](#) where shorter responses are rewarded more while longer incorrect responses go under-penalized. Since Owen values must sum to the total reward (due to the efficiency property), longer sequences experience systematic dilution where each token receives exponentially weaker gradient signals compared to shorter responses. To eliminate this bias, we multiply by sequence length:

$$A_t^{(g)} = T \cdot \tilde{\phi}_t^{(g)} \cdot \hat{A}^{(g)}. \quad (6)$$

This ensures the average token advantage  $\frac{1}{T} \sum_t A_t^{(g)} = \hat{A}^{(g)}$  equals the original sequence-level advantage regardless of length (proof in [Lemma A.1](#), [Section A.1](#) of Appendix), eliminating the length-dependent training bias identified by [Liu et al. \(2025\)](#).

Substituting these **token-specific** advantages  $A_t^{(g)}$  into the GRPO objective (Eq. 3)—which uses uniform sequence-level advantages  $\hat{A}^{(g)}$ —yields the **OSPO objective**<sup>4</sup>:

$$\mathcal{J}^{\text{OSPO}}(\theta) = \frac{1}{G} \sum_{g=1}^G \frac{1}{T} \sum_{t=1}^T \min\left(\rho_t^{(g)} A_t^{(g)}, \text{clip}(\rho_t^{(g)}, 1-\epsilon, 1+\epsilon) A_t^{(g)}\right), \quad (7)$$

where  $A_t^{(g)} = T \cdot \tilde{\phi}_t^{(g)} \cdot \hat{A}^{(g)}$  are Owen-weighted token advantages (cf. Eq. 6). **The key distinction from GRPO:** while GRPO assigns the same advantage  $\hat{A}^{(g)}$  to all tokens in sequence  $g$ , OSPO redistributes this advantage proportionally to each token’s causal contribution  $\phi_t^{(g)}$  as measured by Owen values. Algorithm 1 provides the complete OSPO training procedure.

**Proportional vs. Rank-Based Redistribution.** Equation 6 uses Owen values directly as importance weights—we call this **OSPO-Prop** (proportional). We also explore **OSPO-Rank**, which converts Owen values to ordinal ranks before redistribution, providing robustness when estimates are noisy in long sequences. This spreads credit more uniformly according to relative importance rather than absolute magnitudes. In our experimental setup and results section, we focus on OSPO-PROP as our primary approach, using OSPO-RANK as an ablation study.

**Rank-Based Owen Redistribution.** Instead of redistributing the group advantage  $\hat{A}^{(g)}$  proportionally to the normalized Owen values  $\tilde{\phi}_t^{(g)}$ , we map each token’s Owen value  $\phi_t^{(g)}$  to its ordinal rank position among all tokens in the sequence. Let  $\text{rank}_t^{(g)}$  denote the rank (1 = lowest,  $T =$

<sup>4</sup>We omit the expectation operator for brevity; it is understood that the objective is computed over batches sampled from  $\mathcal{D}$  with rollouts from  $\pi_{\theta_{\text{old}}}$ .

### Algorithm 1 Owen-Shapley Policy Optimization (OSPO)

**Input:** Policy  $\pi_\theta$ , dataset  $\mathcal{D}$ , reward  $r$ , segmentation function  $\text{SEGMENT}(\cdot)$ , coalition width  $w_{\text{max}}$ , samples  $M$ , group size  $G$

- 1: **for**  $x \sim \mathcal{D}$  **do**
- 2:   Sample  $G$  responses  $\{y^{(g)}\}_{g=1}^G \sim \pi_{\theta_{\text{old}}}(\cdot | x)$
- 3:   **for**  $g = 1, \dots, G$  **do**
- 4:     Segment  $\mathcal{A}^{(g)} = \text{SEGMENT}(y^{(g)})$  and compute  $r^{(g)} = r(x, y^{(g)})$
- 5:     Sample  $M$  coalitions  $\{S_m\}_{m=1}^M$  with  $S_m \subseteq \{1, \dots, N\}$ ,  $|S_m| \leq w_{\text{max}}$
- 6:     Compute Owen values:  $\phi_j = \frac{1}{|C_j|} \sum_{S \in C_j} [v(S \cup \{j\}) - v(S)]$
- 7:     Map to tokens:  $\phi_{\text{seg}}^{(g)} = (W^{(g)})^\top \phi_{\text{seg}}$
- 8:     Normalize:  $\tilde{\phi}_t^{(g)} = \phi_t^{(g)} / \sum_{t'} \phi_{t'}^{(g)}$
- 9:     Compute advantage:  $\hat{A}^{(g)} = (r^{(g)} - \bar{r}) / \sigma_r$
- 10:    Redistribute:  $A_t^{(g)} = T \cdot \tilde{\phi}_t^{(g)} \cdot \hat{A}^{(g)}$
- 11:    Compute ratio:  $\rho_t^{(g)} = \pi_\theta(y_t^{(g)} | x, y_{<t}) / \pi_{\theta_{\text{old}}}(y_t^{(g)} | x, y_{<t})$
- 12:   **end for**
- 13:   Update:  $\mathcal{L}_{\text{OSPO}} = \frac{1}{GT} \sum_{g,t} \min(\rho_t^{(g)} A_t^{(g)}, \text{clip}_\epsilon(\rho_t^{(g)}) A_t^{(g)})$
- 14: **end for**

highest) of token  $t$  by its  $\phi_t^{(g)}$  value. The rank-based redistributed advantage is then defined as:

$$A_t^{(g)} = T \cdot \hat{A}^{(g)} \cdot \frac{\text{rank}_t^{(g)}}{\sum_{t'=1}^T \text{rank}_{t'}^{(g)}}. \quad (8)$$

This formulation preserves the same length-invariant property as Eq. 6, ensuring that  $\frac{1}{T} \sum_{t=1}^T A_t^{(g)} = \hat{A}^{(g)}$ , while redistributing credit more uniformly across tokens according to their relative importance rather than absolute Owen magnitudes. Intuitively, OSPO-RANK smooths noisy or highly skewed Owen attributions—useful when a few tokens dominate the proportional weights or when the estimated  $\phi_t$  values are unstable in long sequences.

## 4. Experimental Setup

In this section we outline our experimental settings including tasks/datasets, prompts, metrics, and implementation details.

We evaluate OSPO on two e-commerce tasks testing complementary aspects of advantage redistribution. **Product search query refinement** tests whether models can identify which tokens in expanded queries drive retrieval success—customers provide under-specified queries that LLMs expand with attributes, but standard RL methods assign uniform credit across all tokens despite unequal contributions to retrieval performance. **User profile summarization** tests whether advantage redistribution improves intermediate reasoning quality: models generate purchase history summaries before predicting next items, and since true preferences are latent, summary quality directly determines downstream accuracy. A key design choice: Owen values target the refined query for search tasks but the reasoning trace for summarization, assessing OSPO’s impact across different output types. We use two e-commerce datasets: ESCI shopping queries ([Reddy et al., 2022](#)) for conventional search, H&M Fashion Recommendations ([Ling et al., 2022](#)) for contextualized search and user summarization. Since H&M lacks

explicit queries, we generate them using Claude Sonnet 3.0 from transaction data. Similar to prior work (Lin et al., 2025), all search tasks use dense retrieval via FAISS (Douze et al., 2024) with domain-specific encoders (ALL-MPNET-BASE-v2 for ESCI, SIMCSE-LARGE for H&M). Models generate chain-of-thought reasoning followed by task outputs; see Figure 4 and Figure 5 in Appendix A.4 to see our detailed prompts with examples.

**Expert Data Generation** We first conduct an expert data generation phase using Claude Sonnet 3.0. We sample diverse customer profiles from the H&M Fashion Recommendation dataset (Ling et al., 2022), which provides rich transactional histories but lacks explicit user summaries or search queries. The expert model is then used to generate high-quality synthetic training data for all baselines. For the **contextualized product search** task, the same expert generates naturalistic, history-grounded search queries from the transactions of sampled customers (see Figure 6 for the expert prompt). For the **user profile summarization** task, the expert produces next-purchase predictions (chronologically ordered) to define “winning” and “losing” summaries for preference-tuning methods, while only the high-quality (winning) samples are used for SFT. See Appendix A.3 for details on prompts and evaluation of experts.

**Baselines** We evaluate OSPO against standard fine-tuning and RL baselines—**SFT**, **DPO** (Rafailov et al., 2023a), and **GRPO** (Shao et al., 2024a)—using the same Qwen2.5-Instruct 7B backbone across tasks. SFT is trained on high-quality expert samples filtered by task performance ( $\text{NDCG} \geq 0.5$  for summarization,  $\geq 0.3$  for search), while DPO uses expert contrastive pairs differing by at least 5% in average precision. GRPO serves as the reference value-free RL baseline (Williams, 1992b) using the same reward functions as OSPO—NDCG of the output refined query for search tasks using domain-specific retrievers and a trained Bradley-Terry (Bradley & Terry, 1952; Hong et al., 2024; Nath et al., 2025) loss based reward model based reward scores for the user profile summarization task. We use the Qwen2.5-Instruct 7B model with a reward head on the base LM for learning the reward model from expert generated user summaries described in the next section. For retrieval, we use the best-performing domain encoders from preliminary experiments: ALL-MPNET-BASE-v2 for the ESCI shopping task and SIMCSE-LARGE for the H&M fashion domain. We additionally evaluate **OSPO-Clip**—an ablative variant of OSPO-PROP—which constrains redistributed advantages to  $A_t \in [-2\sigma_{\hat{A}}, +2\sigma_{\hat{A}}]$  based on Chebyshev’s inequality, where  $\sigma_{\hat{A}} = \text{std}(\hat{A}^{(g)})$  is the GRPO baseline standard deviation. Further implementation details and hyperparameters are provided in Appendix A.4.

**Evaluation Settings** We sample responses from trained baselines (including base instruct models) on each task’s evaluation set using temperature 1.0. For product search, performance is measured with retrieval metrics such as

NDCG and average precision with candidate filtering from a pool<sup>5</sup> after initial FAISS-based retrieval. For user profile summarization, we assess sampled summaries via an LLM judge (Qwen-3-Nemotron-32B-Reward (Wang et al., 2025)) using pairwise head-to-head win–loss–tie evaluations, applying a Borda-count (Emerson, 2013) that assigns 1 for a win and  $\frac{1}{2}$  for a tie.

## 5. Results

Results in Table 1 show final performance metrics of various baselines and OSPO variants on product search tasks. OSPO-PROP achieves the best performance among 7B models on all metrics, excelling on ESCI (NDCG 0.522, MRR 0.541) and performing strongly on the harder H&M Fashion dataset (NDCG 0.436, MRR 0.419). While the much larger Qwen-2.5-72B-Instruct baseline achieves marginally higher ESCI scores (NDCG 0.540, MRR 0.560), OSPO-PROP demonstrates that fine-grained credit assignment can approach the performance of models 10x larger at a fraction of the computational cost. These gains hold across retrieval architectures (ALL-MPNET-BASE-v2 for ESCI and SIMCSE-LARGE for H&M), demonstrating OSPO’s adaptability to different embedding spaces and query structures. The performance drop across all models on H&M reflects its higher task complexity, where LLM-generated refined search queries must integrate user preferences as well as their needs, often “latent” in the input queries. Despite this, OSPO retains its lead, suggesting its coalition-based credit assignment effectively captures how query phrasing influences retrieval outcomes in both simple and context-rich recommendation settings.

### Comparison with Online RL and Offline Methods.

Compared to the online RL baseline GRPO, OSPO-Prop achieves 24.9% higher NDCG on ESCI (0.522 vs. 0.418) and 15.0% higher on H&M (0.436 vs. 0.379). This improvement highlights OSPO’s advantage redistribution, which attributes reward more precisely to influential query segments. Over offline alignment methods, OSPO also outperforms DPO by 21.1% on ESCI (0.522 vs. 0.431) and 10.1% on H&M (0.436 vs. 0.396). While SFT and DPO improve upon base models, their lack of retrieval-grounded feedback limits active exploration and the ability to discern which query elements affect ranking. These shortcomings become more pronounced in the contextualized H&M setting, where relevance depends on modeling user-specific preferences, often “latent” in the input query by design. OSPO bridges this gap through principled credit assignment—offering a clear advantage in aligning LLMs with retrieval-oriented objectives.

**Scaling Alone Isn’t Enough.** At just 7B parameters, OSPO-Prop (NDCG 0.522 on ESCI) surpasses the 32B Qwen model (0.496) and approaches the 72B variant (0.543).

<sup>5</sup>We provide details on the candidate pool construction in Appendix Section A.4.

Baseline	ESCI Shopping Queries				H&M Fashion			
	NDCG	AP	MRR	Recall	NDCG	AP	MRR	Recall
Qwen2.5-0.5B	0.379	0.115	0.392	0.116	0.337	0.320	0.320	0.387
Qwen2.5-1.5B	0.439	0.137	0.454	0.138	0.348	0.330	0.330	0.402
Qwen2.5-3B	0.373	0.114	0.387	0.114	0.332	0.317	0.317	0.377
Qwen2.5-32B	0.496	0.158	0.514	0.160	0.438	0.421	0.421	0.490
Qwen2.5-72B	0.543	0.170	0.564	0.171	0.357	0.340	0.340	0.409
SFT (7B)	0.398	0.119	0.411	0.120	0.373	0.355	0.355	0.424
DPO (7B)	0.431	0.133	0.441	0.133	0.396	0.378	0.378	0.449
GRPO (7B)	0.418	0.130	0.430	0.131	0.379	0.366	0.366	0.421
<b>OSPO (Rank) (7B)</b>	<b>0.485</b>	<b>0.158</b>	<b>0.500</b>	<b>0.159</b>	<b>0.399</b>	<b>0.383</b>	<b>0.383</b>	<b>0.445</b>
<b>OSPO (Prop-clip) (7B)</b>	<b>0.495</b>	<b>0.157</b>	<b>0.508</b>	<b>0.159</b>	<b>0.403</b>	<b>0.446</b>	<b>0.389</b>	<b>0.389</b>
<b>OSPO (Prop) (7B)</b>	<b>0.522</b>	<b>0.166</b>	<b>0.541</b>	<b>0.167</b>	<b>0.436</b>	<b>0.419</b>	<b>0.419</b>	<b>0.486</b>

Table 1. Results on ESCI (Reddy et al., 2022) and H&M Fashion Domains (Ling et al., 2022). All baseline generated refined queries are evaluated with dense retrieval using FAISS HNSW indices built over task-specific encoders—ALL-MPNET-BASE-V2 for ESCI and SIMCSE-LARGE for H&M. Top- $K=1000$  retrieval is performed with candidate pools used for filtering relevant candidates post FAISS-based retrieval. We use a temperature of 1.0 with sampling to sample all completions.

Pair	Ties	WR
OSPO-RANK vs DPO	47	45.8
OSPO-RANK vs GRPO	42	47.6
OSPO-RANK vs SFT	40	<b>54.0</b>
OSPO-PROP vs GRPO	38	49.1
OSPO-PROP vs DPO	45	49.6
OSPO-PROP vs SFT	81	<b>53.3</b>

Table 2. Pairwise win-rate performance for user summary generation. Win rate is computed as  $WR_A = (wins_A + 0.5 \text{ ties}) / (wins + losses + ties)$ .

On H&M, it nearly matches the 32B model (0.436 vs. 0.438) while substantially exceeding the 72B model (0.357). These results show that for search and retrieval-oriented generation, refined credit assignment and active exploration in RL is more impactful than raw parameter scaling. Larger models exhibit inconsistent cross-domain performance, with the 72B variant degrading sharply on H&M—evidence that scale alone cannot guarantee robustness without retrieval-aware optimization. OSPO’s coalition-based reward attribution enables efficient learning with far fewer parameters, suggesting that for real-world query refinement tasks, smaller but well-aligned models may offer a better trade-off between accuracy, cost, and deployability.

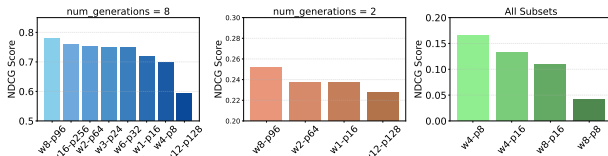


Figure 2. OSPO-PROP ablation results on varying coalition structure on ESCI product search task.  $w$  denotes the maximum coalition span ( $w_{max}$ ) and  $p$  the number of coalitions sampled ( $M$ ) for Owen value estimation in OSPO (Algorithm 1).

**OSPO Demonstrates Superior Generalization** Figure 3 (right) reveals that OSPO (no-clip) exhibits stable improvement on test data throughout training (reaching  $NDCG \approx 0.45$ ), while GRPO shows catastrophic performance collapse around step 400-750. This generalization gap manifests despite GRPO achieving higher training rewards (0.7603 vs. 0.6975 for OSPO), highlighting a “classic overfitting” scenario. Two behavioral markers explain this pattern: First, GRPO (Shao et al., 2024a) *systematically reduces thinking tokens* (roughly around 300th step mark) compared to OSPO variants precisely when test performance degrades (See Figure 3 (left)), while OSPO maintains consistently longer reasoning traces. Second, GRPO’s reward variance drops sharply toward 0.30 by training end, compared to OSPO’s maintained higher variance (0.34-0.36), indicating GRPO converges to consistent but limited solutions that exploit training patterns without transferring to unseen data.

We additionally performed a **cross-retriever evaluation** to assess generalization across embedding spaces at *test time*. In the first setting, RL baselines trained on the ESCI domain with dense rewards from ALL-MPNET-BASE-V2 embeddings were evaluated under a retriever shift using SIMCSE-LARGE. In the reverse setting, these baselines trained on the H&M domain with a SIMCSE-LARGE FAISS index were tested using ALL-MPNET-BASE-V2. To provide a complete comparison, we also evaluated non-RL baselines and base models under the same shifts. As shown in Table 4 in Appendix A.5, OSPO sustains strong ranking performance in both transfer directions, whereas GRPO degrades sharply, confirming that OSPO learns a more transferable and retriever-agnostic alignment signal.

**Coalition Structure Drives OSPO Performance** OSPO’s performance is governed by the interaction between coalition width, exploration depth, and contiguity.

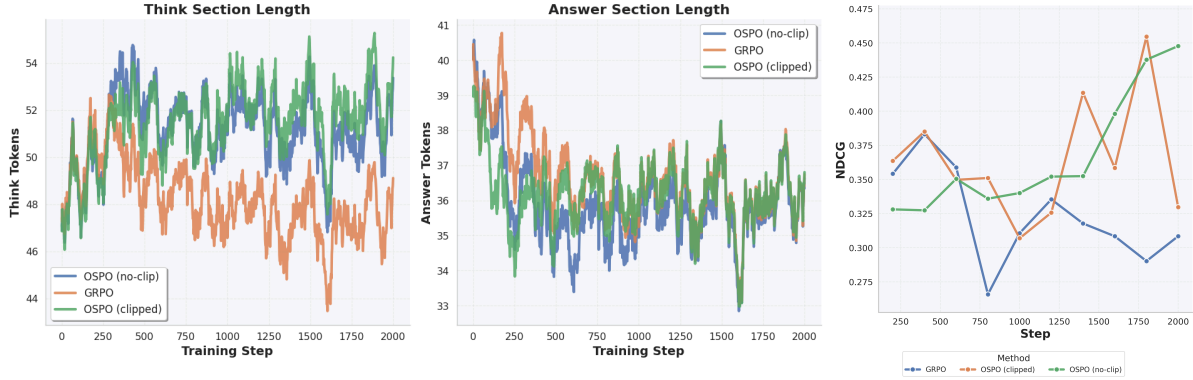


Figure 3. Left and middle: Chain-of-thought (CoT) lengths within `<think>` fields and refined query lengths within `<answer>` fields during RL training of OSPO variants and GRPO on the H&M product search task. Right: evaluation performance on 500 randomly sampled H&M test queries, measured every 200 training steps.

As shown in Fig. Figure 2 (left), moderately wide coalitions (w8–p96) strike the best balance between local compositional context and sampling diversity (NDCG 0.782). Narrow coalitions overfit to token-level co-occurrences, while overly wide coalitions dilute credit assignment and degrade performance (NDCG 0.595). Exploration is equally critical: reducing generations (rollouts) from eight to two (Fig. Figure 2, middle) causes a sharp drop in accuracy, highlighting the need for sufficient Monte Carlo sampling. Finally, removing the contiguity constraint (Fig. Figure 2, right) leads to a dramatic collapse in performance (NDCG 0.113), as non-contiguous coalitions disperse credit across unrelated segments. Overall, OSPO performs best with contiguous, moderately wide coalitions and adequate sampling, yielding more stable and generalizable credit assignment.

**User Profile Quality Analysis.** Table 2 reports pairwise win rates on profile quality, scored by Qwen-3-Nemotron-32B-Reward (Wang et al., 2025), a reward model trained on human preferences with strong performance on Reward-Bench and JudgeBench (Tan et al., 2025). We evaluate on the H&M Fashion dataset (Ling et al., 2022), sampling customer purchase histories to generate profile summaries from each alignment method. Both OSPO-RANK and OSPO-PROP outperform all baselines, with largest margins over SFT (54.0% and 53.3% win rates, +16.8 and +24.4 percentage points vs. baseline). OSPO with Owen-Shapley credit assignment produces higher-quality preference reasoning than SFT, and maintains consistent advantages over DPO and GRPO (45.8–49.6% win rates). Unlike query refinement in both product search tasks where we use phrase-level coalitions, user profile generation employs sentence-level coalitions since complete thoughts better capture distinct aspects of customer preferences (e.g., “prefers sustainable brands” vs. “values affordable basics”). This granularity allows coalition-based value decomposition to yield more coherent profiles than standard RL approaches that assign uniform credit. Modest tie rates with SFT (8.8–17.8%) indicate

both methods handle straightforward cases, while OSPO more reliably wins when distinctions matter. The comparable performance of OSPO-RANK and OSPO-PROP shows both advantage formulations effectively capture intermediate reasoning value. We provide a detailed case study on sentence-level Owen values and actual coalitions in Table 8 to Table 11.

## 6. Conclusion and Future Work

We introduced **Owen-Shapley Policy Optimization (OSPO)**, a reinforcement learning framework that directly tackles the credit assignment problem in language-driven recommendation systems. By decomposing sequence-level rewards into segment-level attributions through cooperative game theory, OSPO enables precise gradient updates without relying on auxiliary value networks. Across product search and user summarization tasks, OSPO consistently outperforms both online and offline baselines, achieving ranking performance comparable to models an order of magnitude larger. This efficiency arises from its attribution-driven optimization, which focuses updates on the sequence segments that meaningfully influence task outcomes. Even with unseen retrievers, OSPO preserves robust performance, showing that its alignment signal transfers across feedback models and representation spaces. Ablation studies further highlight the importance of its coalition structure: moderate-width, contiguous, and sufficiently sampled coalitions act as an intrinsic regularizer that stabilizes learning and improves generalization. In summary, OSPO learns not by memorizing feedback patterns but by leveraging *principled coalition-based attributions that promote stable, transferable, and interpretable behaviors*. Future work can extend these ideas to multi-turn, agentic environments and broader reasoning domains such as code generation, dialogue planning, and interactive decision-making.

**Limitations.** OSPO incurs additional computational overhead compared to standard policy-gradient methods, since

estimating Owen values for advantage redistribution adds extra computation. While FAISS-based retrieval feedback keeps this cost manageable for product search, it becomes more noticeable when using slower reward models, as in user profile summarization. Still, the trade-off is favorable for precision-critical applications where OSPO achieves higher performance and efficiency than much larger models. Several practical challenges remain. Performance is sensitive to coalition width and sampling depth, making hyperparameter tuning crucial but challenging to the practitioner. Additionally, Monte Carlo approximations of Owen values during coalition sampling may underrepresent long-range dependencies between non-adjacent segments, and model stability can vary with feedback quality across domains. Finally, our evaluation spans only two recommendation settings and single-turn RL; extending OSPO to multi-turn, conversational, and multimodal environments remains promising future work.

## References

Ahmadian, A., Cremer, C., Gallé, M., Fadaee, M., Kreutzer, J., Pietquin, O., Üstün, A., and Hooker, S. Back to basics: Revisiting REINFORCE-style optimization for learning from human feedback in LLMs. In Ku, L.-W., Martins, A., and Srikumar, V. (eds.), *Proceedings of the 62nd Annual Meeting of the Association for Computational Linguistics (Volume 1: Long Papers)*, pp. 12248–12267, Bangkok, Thailand, August 2024. Association for Computational Linguistics. doi: 10.18653/v1/2024.acl-long.662. URL <https://aclanthology.org/2024.acl-long.662/>.

Azar, M. G., Guo, Z. D., Piot, B., Munos, R., Rowland, M., Valko, M., and Calandriello, D. A general theoretical paradigm to understand learning from human preferences. In *International Conference on Artificial Intelligence and Statistics*, pp. 4447–4455. PMLR, 2024.

Bai, Y., Jones, A., Ndousse, K., Askell, A., Chen, A., Das-Sarma, N., Drain, D., Fort, S., Ganguli, D., Henighan, T., et al. Training a helpful and harmless assistant with reinforcement learning from human feedback. *arXiv preprint arXiv:2204.05862*, 2022.

Bang, S. and Song, H. Llm-based user profile management for recommender system. *arXiv preprint arXiv:2502.14541*, 2025.

Bradley, R. A. and Terry, M. E. Rank analysis of incomplete block designs: I. the method of paired comparisons. *Biometrika*, 39(3/4):324–345, 1952. doi: 10.2307/2334029.

Cao, M., Zhang, S., Chang, X.-W., and Precup, D. Scar: Shapley credit assignment for more efficient rlhf. *arXiv preprint arXiv:2505.20417*, 2025.

Chai, Y., Sun, H., Fang, H., Wang, S., Sun, Y., and Wu, H. Ma-rlhf: Reinforcement learning from human feedback with macro actions, 2025. URL <https://arxiv.org/abs/2410.02743>.

Chan, A. J., Sun, H., Holt, S., and van der Schaar, M. Dense reward for free in reinforcement learning from human feedback. In *Forty-first International Conference on Machine Learning*, 2024. URL <https://openreview.net/forum?id=eyxVRMrZ4m>.

Cheng, J., Qiao, R., Li, L., Guo, C., Wang, J., Xiong, G., Lv, Y., and Wang, F.-Y. Stop summation: Min-form credit assignment is all process reward model needs for reasoning, 2025. URL <https://arxiv.org/abs/2504.15275>.

Cheng-Guo, E., Li, Q.-L., and Li, S.-Y. The owen value of stochastic cooperative game. *The Scientific World Journal*, 2014:853128, 2014.

Choudhury, S. Process reward models for llm agents: Practical framework and directions, 2025. URL <https://arxiv.org/abs/2502.10325>.

DeepSeek-AI, Guo, D., Yang, D., Zhang, H., Song, J., Zhang, R., Xu, R., Zhu, Q., Ma, S., Wang, P., Bi, X., Zhang, X., Yu, X., Wu, Y., Wu, Z. F., Gou, Z., Shao, Z., Li, Z., Gao, Z., Liu, A., Xue, B., Wang, B., Wu, B., Feng, B., Lu, C., Zhao, C., Deng, C., Zhang, C., Ruan, C., Dai, D., Chen, D., Ji, D., Li, E., Lin, F., Dai, F., Luo, F., Hao, G., Chen, G., Li, G., Zhang, H., Bao, H., Xu, H., Wang, H., Ding, H., Xin, H., Gao, H., Qu, H., Li, H., Guo, J., Li, J., Wang, J., Chen, J., Yuan, J., Qiu, J., Li, J., Cai, J. L., Ni, J., Liang, J., Chen, J., Dong, K., Hu, K., Gao, K., Guan, K., Huang, K., Yu, K., Wang, L., Zhang, L., Zhao, L., Wang, L., Zhang, L., Xu, L., Xia, L., Zhang, M., Zhang, M., Tang, M., Li, M., Wang, M., Li, M., Tian, N., Huang, P., Zhang, P., Wang, Q., Chen, Q., Du, Q., Ge, R., Zhang, R., Pan, R., Wang, R., Chen, R. J., Jin, R. L., Chen, R., Lu, S., Zhou, S., Chen, S., Ye, S., Wang, S., Yu, S., Zhou, S., Pan, S., and Li, S. S. Deepseek-r1: Incentivizing reasoning capability in llms via reinforcement learning. *CoRR*, abs/2501.12948, 2025.

Douze, M., Guzhva, A., Deng, C., Johnson, J., Szilvassy, G., Mazaré, P.-E., Lomeli, M., Hosseini, L., and Jégou, H. The faiss library. *arXiv preprint arXiv:2401.08281*, 2024.

Emerson, P. The original borda count and partial voting. *Social Choice and Welfare*, 40(2):353–358, 2013.

Fang, M., Wan, X., Lu, F., Xing, F., and Zou, K. Mathodyssey: Benchmarking mathematical problem-solving

skills in large language models using odyssey math data. *Scientific Data*, 12(1):1392, 2025.

Gao, Y., Sheng, T., Xiang, Y., Xiong, Y., Wang, H., and Zhang, J. Chat-rec: Towards interactive and explainable llms-augmented recommender system, 2023. URL <https://arxiv.org/abs/2303.14524>.

Geng, S., Liu, S., Fu, Z., Ge, Y., and Zhang, Y. Recommendation as language processing (rlp): A unified pretrain, personalized prompt & predict paradigm (p5), 2023. URL <https://arxiv.org/abs/2203.13366>.

Giménez Pradales, J. M. and Puente del Campo, M. A. The owen and the owen-banzhaf values applied to the study of the madrid assembly and the andalusian parliament in legislature 2015-2019. In *Proceedings of the 8th International Conference on Operations Research and Enterprise Systems-Volume 1: ICORES, 45-52, 2019, Prague, Czech Republic*, pp. 45–52. Scitepress, 2019.

Goldshmidt, R. and Horovitz, M. Tokenshap: Interpreting large language models with monte carlo shapley value estimation. *arXiv preprint arXiv:2407.10114*, 2024.

He, Y., Wang, Z., Shen, Z., Sun, G., Dai, Y., Wu, Y., Wang, H., and Li, A. Shed: Shapley-based automated dataset refinement for instruction fine-tuning. *arXiv preprint arXiv:2405.00705*, 2024.

Henderson, P., Islam, R., Bachman, P., Pineau, J., Precup, D., and Meger, D. Deep reinforcement learning that matters. In *Proceedings of the AAAI conference on artificial intelligence*, volume 32, 2018.

Hong, J., Lee, N., and Thorne, J. ORPO: Monolithic preference optimization without reference model. In *Proceedings of the 2024 Conference on Empirical Methods in Natural Language Processing*, pp. 11170–11189, 2024.

Jeong, J., Chow, Y., Tennenholz, G., Hsu, C.-W., Tulepbergenov, A., Ghavamzadeh, M., and Boutilier, C. Factual and personalized recommendations using language models and reinforcement learning. *arXiv preprint arXiv:2310.06176*, 2023.

Kazemnejad, A., Aghajohari, M., Portelance, E., Sordoni, A., Reddy, S., Courville, A., and Le Roux, N. Vineppo: Unlocking rl potential for llm reasoning through refined credit assignment. 2024.

Konidaris, G. and Barto, A. Skill discovery in continuous reinforcement learning domains using skill chaining. *Advances in neural information processing systems*, 22, 2009.

Koo, R., Yang, I., Raheja, V., Hong, M., Jun, K.-S., and Kang, D. Learning explainable dense reward shapes via bayesian optimization. *arXiv preprint arXiv:2504.16272*, 2025.

Kool, W., van Hoof, H., and Welling, M. Buy 4 REINFORCE samples, get a baseline for free!, 2019. URL <https://openreview.net/forum?id=r11gTGL5DE>.

Langley, P. Crafting papers on machine learning. In Langley, P. (ed.), *Proceedings of the 17th International Conference on Machine Learning (ICML 2000)*, pp. 1207–1216, Stanford, CA, 2000. Morgan Kaufmann.

Li, Y., Ma, S., Wang, X., Huang, S., Jiang, C., Zheng, H.-T., Xie, P., Huang, F., and Jiang, Y. Ecomgpt: Instruction-tuning large language models with chain-of-task tasks for e-commerce, 2023. URL <https://arxiv.org/abs/2308.06966>.

Lightman, H., Kosaraju, V., Burda, Y., Edwards, H., Baker, B., Lee, T., Leike, J., Schulman, J., Sutskever, I., and Cobbe, K. Let's verify step by step. In *The Twelfth International Conference on Learning Representations*, 2023.

Lin, J., Wang, T., and Qian, K. Rec-r1: Bridging generative large language models and user-centric recommendation systems via reinforcement learning. *arXiv preprint arXiv:2503.24289*, 2025.

Ling, C. G., ElizabethHMGroup, FridaRim, inversion, Ferrando, J., Maggie, neuraloverflow, and xlsrln. Hm personalized fashion recommendations. <https://kaggle.com/competitions/h-and-m-personalized-fashion-recommendations>, 2022. Kaggle.

Liu, H., Mao, X., Xia, H., Lou, J., and Liu, J. Prompt valuation based on shapley values. *arXiv preprint arXiv:2312.15395*, 2023a.

Liu, S., Cai, Q., Sun, B., Wang, Y., Jiang, J., Zheng, D., Jiang, P., Gai, K., Zhao, X., and Zhang, Y. Exploration and regularization of the latent action space in recommendation. In *Proceedings of the ACM Web Conference 2023*, pp. 833–844, 2023b.

Liu, Z., Chen, C., Li, W., Qi, P., Pang, T., Du, C., Lee, W. S., and Lin, M. Understanding r1-zero-like training: A critical perspective, 2025. URL <https://arxiv.org/abs/2503.20783>.

Lu, W., Lian, J., Zhang, W., Li, G., Zhou, M., Liao, H., and Xie, X. Aligning large language models for controllable recommendations. *arXiv preprint arXiv:2403.05063*, 2024.

Lundberg, S. M. and Lee, S.-I. A unified approach to interpreting model predictions. *Advances in neural information processing systems*, 30, 2017.

Luo, S., He, B., Zhao, H., Shao, W., Qi, Y., Huang, Y., Zhou, A., Yao, Y., Li, Z., Xiao, Y., Zhan, M., and Song, L. Recranker: Instruction tuning large language model as ranker for top-k recommendation, 2024. URL <https://arxiv.org/abs/2312.16018>.

Mohammadi, B. Explaining large language models decisions using shapley values. *arXiv preprint arXiv:2404.01332*, 2024.

Nath, A., Volozin, A., Saha, S., Nanda, A. A., Grunin, G., Bhotika, R., and Krishnaswamy, N. Dpl: Diverse preference learning without a reference model. In *Proceedings of the 2025 Conference of the North American Chapter of the Association for Computational Linguistics: Human Language Technologies (NAACL 2025)*, January 2025. Last modified: 24 Feb 2025.

Ng, A. Y., Harada, D., and Russell, S. Policy invariance under reward transformations: Theory and application to reward shaping. In *Icml*, volume 99, pp. 278–287. Citeseer, 1999.

Owen, A. B. Sobol'indices and shapley value. *SIAM/ASA Journal on Uncertainty Quantification*, 2(1):245–251, 2014.

Owen, G. Values of games with a priori unions. In *Mathematical economics and game theory: Essays in honor of Oskar Morgenstern*, pp. 76–88. Springer, 1977.

Parthasarathi, P., Reymond, M., Chen, B., Cui, Y., and Chandar, S. Grpo- $\lambda$ : Credit assignment improves llm reasoning, 2025. URL <https://arxiv.org/abs/2510.00194>.

Peng, Q., Liu, H., Huang, H., Yang, Q., and Shao, M. A survey on llm-powered agents for recommender systems, 2025. URL <https://arxiv.org/abs/2502.10050>.

Pignatelli, E., Ferret, J., Paglieri, D., Coward, S., Rocktäschel, T., Grefenstette, E., and Toni, L. Assessing the zero-shot capabilities of llms for action evaluation in rl. In *Automated Reinforcement Learning: Exploring Meta-Learning, AutoML, and LLMs*.

Rafailov, R., Sharma, A., Mitchell, E., Ermon, S., Manning, C. D., and Finn, C. Direct preference optimization: Your language model is secretly a reward model. In *NeurIPS*, 2023a.

Rafailov, R., Sharma, A., Mitchell, E., Manning, C. D., Ermon, S., and Finn, C. Direct preference optimization: Your language model is secretly a reward model. *Proceedings of the Annual Conference on Neural Information Processing Systems (NeurIPS)*, 2023b.

Rafailov, R., Hejna, J., Park, R., and Finn, C. From r to  $q^*$ : Your language model is secretly a q-function. *arXiv preprint arXiv:2404.12358*, 2024.

Reddy, C. K., Márquez, L., Valero, F., Rao, N., Zaragoza, H., Bandyopadhyay, S., Biswas, A., Xing, A., and Subbian, K. Shopping queries dataset: A large-scale ESCI benchmark for improving product search. 2022.

Ruess, H. Fairness analysis with shapley-owen effects, 2024. URL <https://arxiv.org/abs/2409.19318>.

Samineni, S. R., Kalwar, D., Valmeekam, K., Stechly, K., and Kambhampati, S. Rl in name only? analyzing the structural assumptions in rl post-training for llms, 2025. URL <https://arxiv.org/abs/2505.13697>.

Schulman, J., Wolski, F., Dhariwal, P., Radford, A., and Klimov, O. Proximal policy optimization algorithms, 2017. URL <https://arxiv.org/abs/1707.06347>.

Shao, Z., Wang, P., Zhu, Q., Xu, R., Song, J., Bi, X., Zhang, H., Zhang, M., Li, Y., Wu, Y., et al. Deepseekmath: Pushing the limits of mathematical reasoning in open language models. *arXiv preprint arXiv:2402.03300*, 2024a.

Shao, Z., Wang, P., Zhu, Q., Xu, R., Song, J., Zhang, M., Li, Y. K., Wu, Y., and Guo, D. Deepseekmath: Pushing the limits of mathematical reasoning in open language models. *CoRR*, abs/2402.03300, 2024b.

Shapley, L. S. Stochastic games. *Proceedings of the national academy of sciences*, 39(10):1095–1100, 1953.

Skalse, J., Howe, N. H. R., Krasheninnikov, D., and Krueger, D. Defining and characterizing reward hacking, 2025. URL <https://arxiv.org/abs/2209.13085>.

Stiennon, N., Ouyang, L., Wu, J., Ziegler, D. M., Lowe, R., Voss, C., Radford, A., Amodei, D., and Christiano, P. Learning to summarize from human feedback, 2020.

Sun, C., Liang, Y., Yang, Y., Xu, S., Yang, T., and Tong, Y. Rlrf4rec: Reinforcement learning from recsys feedback for enhanced recommendation reranking. *arXiv e-prints*, pp. arXiv–2410, 2024.

Sun, C., Yu, H., and Cui, L. Efficient shapley value-based non-uniform pruning of large language models. *arXiv preprint arXiv:2505.01731*, 2025a.

Sun, H., Min, Y., Chen, Z., Zhao, W. X., Fang, L., Liu, Z., Wang, Z., and Wen, J.-R. Challenging the boundaries of reasoning: An olympiad-level math benchmark for

large language models, 2025b. URL <https://arxiv.org/abs/2503.21380>.

Sutton, R. S. *Temporal credit assignment in reinforcement learning*. University of Massachusetts Amherst, 1984.

Sutton, R. S. and Barto, A. G. *Reinforcement learning: An introduction*. MIT press, 2018.

Tan, S., Zhuang, S., Montgomery, K., Tang, W. Y., Cuadron, A., Wang, C., Popa, R. A., and Stoica, I. Judgebench: A benchmark for evaluating llm-based judges, 2025. URL <https://arxiv.org/abs/2410.12784>.

Wang, P., Fan, Y., Xia, L., Zhao, W. X., Niu, S., and Huang, J. Kerl: A knowledge-guided reinforcement learning model for sequential recommendation. In *Proceedings of the 43rd International ACM SIGIR conference on research and development in Information Retrieval*, pp. 209–218, 2020.

Wang, Z., Zeng, J., Delalleau, O., Shin, H.-C., Soares, F., Bukharin, A., Evans, E., Dong, Y., and Kuchaiev, O. HelpSteer3-Preference: Open human-annotated preference data across diverse tasks and languages, 2025. URL <https://arxiv.org/abs/2505.11475>.

Williams, R. J. Simple statistical gradient-following algorithms for connectionist reinforcement learning. *Machine learning*, pp. 229–256, 1992a.

Williams, R. J. Simple statistical gradient-following algorithms for connectionist reinforcement learning. *Mach. Learn.*, 8(3–4):229–256, may 1992b. ISSN 0885-6125. doi: 10.1007/BF00992696. URL <https://doi.org/10.1007/BF00992696>.

Winter, E. The consistency and potential for values of games with coalition structure. *Games and Economic Behavior*, 4(1):132–144, 1992.

Wu, J., Ning, L., Liu, L., Lee, H., Wu, N., Wang, C., Prakash, S., O’Banion, S., Green, B., and Xie, J. Rlpf: Reinforcement learning from prediction feedback for user summarization with llms, 2025. URL <https://arxiv.org/abs/2409.04421>.

Wu, Z., Hu, Y., Shi, W., Dziri, N., Suhr, A., Ammanabrolu, P., Smith, N. A., Ostendorf, M., and Hajishirzi, H. Fine-grained human feedback gives better rewards for language model training. *arXiv preprint arXiv:2306.01693*, 2023.

Xi, Y., Liu, W., Lin, J., Cai, X., Zhu, H., Zhu, J., Chen, B., Tang, R., Zhang, W., and Yu, Y. Towards open-world recommendation with knowledge augmentation from large language models. In *Proceedings of the 18th ACM Conference on Recommender Systems*, pp. 12–22, 2024.

Xi, Y., Lin, J., Xiao, Y., Zhou, Z., Shan, R., Gao, T., Zhu, J., Liu, W., Yu, Y., and Zhang, W. A survey of llm-based deep search agents: Paradigm, optimization, evaluation, and challenges, 2025. URL <https://arxiv.org/abs/2508.05668>.

Xie, G., Shi, Y., Tian, H., Yao, T., and Zhang, X. Capo: Towards enhancing llm reasoning through generative credit assignment, 2025. URL <https://arxiv.org/abs/2508.02298>.

Yao, S., Zhao, J., Yu, D., Du, N., Shafran, I., Narasimhan, K. R., and Cao, Y. React: Synergizing reasoning and acting in language models. In *The eleventh international conference on learning representations*, 2022.

Yue, Y., Yuan, Y., Yu, Q., Zuo, X., Zhu, R., Xu, W., Chen, J., Wang, C., Fan, T., Du, Z., et al. Vapo: Efficient and reliable reinforcement learning for advanced reasoning tasks. *arXiv preprint arXiv:2504.05118*, 2025.

Zhao, X., Zhang, L., Ding, Z., Xia, L., Tang, J., and Yin, D. Recommendations with negative feedback via pairwise deep reinforcement learning. In *Proceedings of the 24th ACM SIGKDD international conference on knowledge discovery & data mining*, pp. 1040–1048, 2018.

Zheng, L., Chiang, W.-L., Sheng, Y., Zhuang, S., Wu, Z., Zhuang, Y., Lin, Z., Li, Z., Li, D., Xing, E. P., Zhang, H., Gonzalez, J. E., and Stoica, I. Judging llm-as-a-judge with mt-bench and chatbot arena, 2023. URL <https://arxiv.org/abs/2306.05685>.

Zhou, K., Zhou, Y., Zhao, W. X., Wang, X., and Wen, J.-R. Towards topic-guided conversational recommender system. In Scott, D., Bel, N., and Zong, C. (eds.), *Proceedings of the 28th International Conference on Computational Linguistics*, pp. 4128–4139, Barcelona, Spain (Online), December 2020. International Committee on Computational Linguistics. doi: 10.18653/v1/2020.coling-main.365. URL <https://aclanthology.org/2020.coling-main.365/>.

## A. Appendices

### A.1. More Details on OSPO Objectives

**Lemma A.1** (Length-Invariant Owen Redistribution). *Let  $y^{(g)}$  be a generated sequence of length  $T$  from a Monte Carlo rollout with reward  $R^{(g)}$ . Following the REINFORCE algorithm (Williams, 1992b; Kool et al., 2019; Shao et al., 2024a) of sampling rollouts without replacement with baseline subtraction, define the sequence-level advantage as:*

$$\hat{A}^{(g)} = R^{(g)} - \bar{R}, \quad \text{where } \bar{R} = \frac{1}{G} \sum_{g'=1}^G R^{(g')}, \quad (9)$$

is the mean reward across  $G$  sampled rollouts. Let  $\{\phi_t^{(g)}\}_{t=1}^T$  denote Owen values satisfying the efficiency axiom  $\sum_{t=1}^T \phi_t^{(g)} = R^{(g)}$  (Cheng-Guo et al., 2014; Owen, 2014). Define the normalized Owen values as  $\tilde{\phi}_t^{(g)} = \phi_t^{(g)} / \sum_{t'=1}^T \phi_{t'}^{(g)}$ , and the redistributed token advantages as:

$$A_t^{(g)} = T \cdot \tilde{\phi}_t^{(g)} \cdot \hat{A}^{(g)}. \quad (10)$$

Then the average token advantage equals the original sequence-level advantage, independent of sequence length:

$$\frac{1}{T} \sum_{t=1}^T A_t^{(g)} = \hat{A}^{(g)}. \quad (11)$$

*Proof.* To prove this, starting from the definition of the redistributed token advantages, we compute the average:

$$\frac{1}{T} \sum_{t=1}^T A_t^{(g)} = \frac{1}{T} \sum_{t=1}^T \left( T \cdot \tilde{\phi}_t^{(g)} \cdot \hat{A}^{(g)} \right) \quad (12)$$

$$= \frac{T}{T} \cdot \hat{A}^{(g)} \sum_{t=1}^T \tilde{\phi}_t^{(g)} \quad (13)$$

$$= \hat{A}^{(g)} \sum_{t=1}^T \tilde{\phi}_t^{(g)}. \quad (14)$$

Now we evaluate the sum of normalized Owen values. By the definition of  $\tilde{\phi}_t^{(g)}$ :

$$\sum_{t=1}^T \tilde{\phi}_t^{(g)} = \sum_{t=1}^T \frac{\phi_t^{(g)}}{\sum_{t'=1}^T \phi_{t'}^{(g)}} \quad (15)$$

$$= \frac{1}{\sum_{t'=1}^T \phi_{t'}^{(g)}} \sum_{t=1}^T \phi_t^{(g)} \quad (16)$$

$$= \frac{\sum_{t=1}^T \phi_t^{(g)}}{\sum_{t'=1}^T \phi_{t'}^{(g)}} \quad (17)$$

$$= \frac{\sum_{t=1}^T \phi_t^{(g)}}{\sum_{t=1}^T \phi_t^{(g)}} \quad (18)$$

$$= 1. \quad (19)$$

Substituting this result back into equation (3), we obtain:

$$\frac{1}{T} \sum_{t=1}^T A_t^{(g)} = \hat{A}^{(g)} \cdot 1 = \hat{A}^{(g)}. \quad (20)$$

This equality holds for any sequence length  $T > 0$ , proving that the redistribution scheme is length-invariant.  $\square$

*Remark A.2.* Lemma A.1 guarantees three critical properties for OSPO’s credit assignment:

1. **Scale Preservation:** The average token advantage matches the original sequence-level advantage  $\hat{A}^{(g)} = R^{(g)} - \bar{R}$ , ensuring gradient magnitudes in Equation (7) remain comparable across sequences of different lengths.
2. **Length Invariance:** A sequence’s total gradient contribution depends on its advantage  $\hat{A}^{(g)}$  and Owen-based credit distribution  $\{\tilde{\phi}_t^{(g)}\}$ , not its verbosity. This eliminates the length bias where longer sequences (e.g., detailed user summaries with  $T > 100$ ) would otherwise receive disproportionately small gradient signals when Owen values are naively redistributed.
3. **Credit Prioritization:** High-value tokens (e.g., product-specific attributes) receive proportionally more advantage than low-value tokens (e.g., filler words or inconsistent reasoning), while maintaining consistency with the per-token policy gradient formulation. Specifically, if  $\tilde{\phi}_i > \tilde{\phi}_j$ , then  $A_i^{(g)} > A_j^{(g)}$ , preserving the ordinal ranking of token contributions.

*Remark A.3* (Connection to the Efficiency Axiom). The normalization step  $\tilde{\phi}_t = \phi_t / \sum_{t'} \phi_{t'}$  is essential because Owen values satisfy the efficiency axiom:  $\sum_{t=1}^T \phi_t = R^{(g)}$  (the terminal reward). Without the length multiplication factor  $T$ , a naive proportional redistribution  $\tilde{A}_t = \hat{A}^{(g)} \cdot \tilde{\phi}_t$  would yield an average advantage of:

$$\frac{1}{T} \sum_{t=1}^T \tilde{A}_t = \frac{\hat{A}^{(g)}}{T} \sum_{t=1}^T \tilde{\phi}_t = \frac{\hat{A}^{(g)}}{T}, \quad (21)$$

introducing a  $1/T$  dilution effect where longer sequences receive significantly weaker gradient signals. The multiplication by  $T$  precisely counteracts this dilution, ensuring that gradient magnitude depends on the quality of the generation (via  $\hat{A}^{(g)}$ ) rather than its length.

## A.2. Length-Invariant Credit Redistribution for GRPO

Group Relative Policy Optimization (GRPO) (Shao et al., 2024a) computes sequence-level advantages by normalizing rewards within a sampled group, but assigns this advantage uniformly to all tokens in the sequence. This uniform assignment creates a fundamental tension: when combined with the standard per-token gradient normalization  $\frac{1}{|y|}$ , GRPO exhibits length-dependent bias where positive advantages produce stronger gradients for shorter sequences, while negative advantages under-penalize verbose failures (Liu et al., 2025). This bias is particularly problematic in recommendation tasks where response length varies significantly—from terse product queries to detailed user preference summaries.

Our approach leverages Owen-Shapley values to redistribute the sequence-level GRPO advantage to individual tokens while explicitly eliminating length bias. Given a sequence  $y$  with GRPO advantage  $\hat{A}$  and Owen values  $\{\Phi_t\}_{t=1}^{|y|}$  (obtained via the efficient approximation in Section 3.1), we face a redistribution challenge. A naive proportional approach would compute token advantages as  $\tilde{A}_t = \hat{A} \cdot \frac{\Phi_t}{\sum_{t'} \Phi_{t'}}$ . However, since Owen values satisfy the efficiency axiom ( $\sum_t \Phi_t = R$ , where  $R$  is the terminal reward), this denominator equals the reward  $R$ , causing per-token advantages to scale as  $\hat{A}/R$ . For sequences with correlated advantages and rewards, this creates the same length bias as vanilla GRPO, where the average token advantage  $\frac{1}{|y|} \sum_t \tilde{A}_t \propto \frac{1}{|y|}$ .

To eliminate this dependency, we propose **two** redistribution strategies that multiply the proportional allocation by sequence length  $|y|$ , ensuring the average token advantage equals the original GRPO advantage regardless of sequence length. This length normalization is critical: it decouples gradient magnitude from verbosity while preserving Owen-based prioritization of important tokens.

**Proportional Owen Redistribution.** Our first approach uses Owen values directly as importance weights:

$$\tilde{A}_t^{\text{prop}} = \hat{A} \cdot \frac{\Phi_t}{\sum_{t'} \Phi_{t'}} \cdot |y| \quad (22)$$

This strategy assigns credit proportional to each token’s marginal contribution, as quantified by its Owen value. Tokens in high-value<sup>6</sup> phrases (e.g., “noise cancelling” in a headphone query) receive proportionally more advantage than tokens

<sup>6</sup>We assume that we have access to a reasonably efficient and realistic retrieval system that is more likely pull up relevant articles for product-specific attributes, while lowering those of filler words.

in low-value phrases (e.g., filler words). The length multiplication ensures that  $\frac{1}{|y|} \sum_t \tilde{A}_t^{\text{prop}} = \hat{A}$ , making the average token advantage independent of sequence length. Our experiments in product search tasks suggests that this redistribution is particularly effective when Owen values accurately reflect token importance—typically in short sequences with clear, attributable contributions.

**Rank-Based Owen Redistribution.** Our second approach converts Owen values to ordinal ranks before redistribution:

$$\text{rank}_t = \text{argsort}(\{\Phi_{t'}\}), \quad \tilde{A}_t^{\text{rank}} = \hat{A} \cdot \frac{\text{rank}_t}{\sum_{t'} \text{rank}_{t'}} \cdot |y| \quad (23)$$

This rank transformation acts as a form of regularization on the Owen-based credit assignment. While proportional redistribution can concentrate credit heavily on a few high-value tokens (e.g., one token receiving 80% of the advantage), rank-based redistribution spreads credit more uniformly according to relative importance order. For a sequence of length  $N$ , the top-ranked token receives weight  $\frac{N-1}{\sum_{k=0}^{N-1} k} = \frac{2}{N}$  instead of a potentially much larger proportion. This uniform spreading is advantageous in two scenarios: (1) when Owen value estimates are noisy due to complex token interactions in long sequences, the ordinal transformation filters magnitude errors while preserving relative importance; (2) when task success requires multiple complementary components (e.g., multiple attributes in a product query), rank-based redistribution prevents over-concentration on a single dominant feature and encourages the model to improve all relevant tokens.

Both strategies maintain the theoretical guarantees of potential-based reward shaping (Ng et al., 1999). The choice between proportional and rank-based redistribution depends on the task structure: proportional excels when token contributions are clearly separable and accurately measurable, while rank-based provides robustness when contributions are compositional and interdependent.

### A.3. Expert Data Generation

Unlike ESCI (Reddy et al., 2022), the H&M Fashion Recommendation dataset (Ling et al., 2022) lacks explicit customer queries—crucial for evaluating search-oriented LLMs. To ensure a fair comparison of OSPO with SFT, preference-tuning, and RL baselines (e.g., GRPO), we conduct an **expert data generation phase** using Claude Sonnet 3.0. The expert model synthesizes missing annotations from sampled customer profiles drawn from rich transactional histories. Specifically, it produces (i) next-purchase predictions and preference-grounded summaries for the *user summarization* task, and (ii) naturalistic, history-conditioned queries for the *contextualized product search* task (see Figure 6). The full pipeline proceeds as follows.

**Customer Data Preparation.** We construct a sequential recommendation dataset by segmenting each customer’s purchase history into temporally ordered windows. A customer is retained if they have at least five prior and four subsequent purchases, providing adequate temporal context while including light users. To maintain computational efficiency, we subsample a fixed number of eligible customers, yielding a balanced and diverse training cohort.

**Expert Data Generation.** Following prior work on RL-based sequential recommendation (Wu et al., 2025), we generate *expert user summaries* that compress behavioral histories into concise representations. Because no ground truth exists for such summaries or reasoning trails, the expert LLM produces Chain-of-Thought (CoT) explanations grounded in observed behavior—capturing both short- and long-term preferences. Unlike Wu et al. (2025), which predicts only the next item, our expert forecasts entire future sequences, pruning implausible candidates while reasoning over temporal dependencies. These CoT traces form structured summaries encoding customer intent and preference dynamics.

**SFT and DPO Trajectories for User Profile Summarization.** From the generated expert data, we construct SFT and DPO (Rafailov et al., 2023a) training sets based on the expert’s performance in sequential purchase prediction, where future items are ranked in temporal order. To ensure data quality, we retain only samples where the expert’s NDCG exceeds a threshold  $T = 0.5$ , tuned empirically. These high-performing traces constitute the SFT data. For DPO, we obtain contrastive pairs by sampling two reasoning traces per example—keeping the higher-NDCG trace as the “winning” response and the lower one as the “losing” response. This consistent expert-driven generation enables fair comparative analysis across SFT, DPO, and RL-based methods trained under identical supervision signals.

**Contextualized Query Generation** For the contextualized product search task, we prompt the same expert model to generate realistic, user-grounded fashion queries conditioned on each customer’s purchase history and item context. Using

Metric	GPT-4o	Claude-Sonnet Run 1	Claude-Sonnet Run 2
Hit@1	0.2622	0.2719	0.2715
MRR	0.4995	0.5021	0.5056
NDCG	0.7413	0.7394	0.7412
Spearman	0.4747	0.4723	0.4708
Hit@3	0.6615	0.6593	0.6729
MRR@3	0.4393	0.4406	0.4458
NDCG@3	0.5970	0.5951	0.5990
Hit@5	0.8095	0.8218	0.8305
MRR@5	0.4730	0.4773	0.4817
NDCG@5	0.6683	0.6680	0.6719
Hit@7	0.9179	0.9272	0.9377
MRR@7	0.4901	0.4938	0.4985
NDCG@7	0.7125	0.7118	0.7166
Hit@9	0.9835	0.9834	0.9843
MRR@9	0.4979	0.5005	0.5041
NDCG@9	0.7359	0.7342	0.7364

Table 3. Overall averages across 5700 samples from the H&M Fashion Recommendations data (Ling et al., 2022) for expert data generation on user summary generation on H&M Fashion Recommendations data. Expert models are instructed to reason about the user’s preferences based on their purchase history, before predicting the next purchases items, conditioned on this reasoning trace.

the role-based prompt in Figure 6, the expert produces diverse, natural-language queries that mimic how real users express shopping intent—balancing explicit style and brand references with implicit preferences, seasonal cues, and underspecified needs. Each generated query is paired with a detailed item rationale, enabling the resulting dataset to capture nuanced intent representations crucial for training and evaluating OSPO on fashion-specific retrieval tasks.

**Prompt Construction** To instantiate this task for large language models, we construct prompts that embed both the historical prefix and the candidate future set. Each prompt begins with an explicit task description, e.g., “*You are an expert sequential recommendation system. Given the customer’s purchase history and buying behavior, predict the exact order in which the customer will buy the next few products.*” This instruction enforces that the output must be a **complete ordering** rather than isolated recommendations, capturing temporal and long-range dependencies in the user behavior. The history is then serialized in natural language with timestamps, prices, and product descriptions (e.g., “*Transaction 3: 2018-12-20 — Price: \$0.01 — Russell Tube — Scarf in Beige ...*”), providing temporal and semantic context, similar to (Wu et al., 2025). Candidate items are presented as a numbered list with their article IDs and textual metadata. The model is asked to “*rank all candidate products in chronological order, with the leftmost article ID being purchased first.*” Finally, to encourage structured reasoning, we include a chain-of-thought directive: “*Please think step by step about the purchase sequence and output your sequential reasoning within <think> and </think> tokens.*” The LLM then outputs a structured list of ranked purchase items—which can be directly aligned with ground-truth chronological list of items for automatic and verifiable evaluation.

#### A.4. Additional Experimental Details

**Task-specific Prompts** Figure 5 and Figure 4 shows the full prompts used for training and evaluation of the conventional product search task (ESCI) and contextualized product search task (H&M Fashion Recommendations). Table 8 shows the full prompt used for user profile summary generation on H&M Fashion data.

**Baselines.** All trainable baselines—**SFT**, **DPO**, **GRPO**, and **OSPO**—use the **Qwen2.5-Instruct 7B** model as the base architecture. For each domain, we also evaluate non-trainable encoder-based retrieval systems as task-specific baselines for contextualized search. Based on preliminary experiments, we selected ALL-MPNET-BASE-V2 for the ESCI shopping task and SIMCSE-LARGE for the fashion domain, as they achieved the highest retrieval NDCG on their respective validation splits when used for FAISS-based dense retrieval.

**Supervised Finetuning (SFT)** is trained using expert-generated samples filtered by task performance, retaining only those with  $\text{NDCG} \geq 0.5$  for user summarization and  $\geq 0.3$  for search tasks. **Direct Preference Optimization (DPO)** (Rafailov et al., 2023a) learns from contrastive pairs sampled from the same expert generation process: “winning” responses are those with higher evaluation scores (NDCG or AP), and “losing” ones are those at least 5% lower in AP or NDCG. **Group-Relative Policy Optimization (GRPO)** (Shao et al., 2024a) is used as the representative value-free RL baseline,

**System Prompt:** You are an expert in query expansion for product retrieval. Your task: enrich the customers query with product attributes and context that improve dense retrieval accuracy. **Important: RETAIN the original query terms and ADD relevant product details.** Your expansion should be a natural phrase combining the original query with product attributes.

**Strategy:**

1. Keep all original query terms
2. Add product category if not explicit (e.g., "laptop" for vague queries)
3. Include key distinguishing attributes: brand, model, specs, materials, use-case

Your expansion should be a natural phrase combining the original query with product attributes, NOT a first-person request. Format your response as follows: First, analyze the query in `<think>` tags: What product category is this? What key attributes would help distinguish the right item from similar products? What buyer intent or use-case is implied?

Then, output your enriched search query in `<answer>` tags as a natural phrase combining the original query with product attributes.

**User Input:** `<INPUT QUERY> (smith and wesson 642 holster)`

*Figure 4.* Full prompt used for training and evaluation on the ESCI product search dataset (Reddy et al., 2022). Following (Lin et al., 2025), we simplify the format by directly requesting the refined query within `<answer>` fields instead of JSON-style `<query>` tags. Only the text within `<answer>` tags is used for Owen value computations in OSPO, while the `<think>` section supports intermediate CoT reasoning. The example query shown in **purple** is drawn from the dataset.

employing identical scalar reward functions as OSPO: retrieval NDCG for contextualized search and reward model scores for user summarization. This unified setup ensures that all baselines differ only in how they learn from expert-generated feedback—contrastively (DPO), directly (SFT), or via sequence-level gradient updates (GRPO/OSPO).

**Format Rewards for User Summarization** While search tasks use only retrieval-based NDCG rewards, the user summarization task benefits from additional format validation. For this task, both OSPO and GRPO use a combined scalar reward with two components: a Bradley–Terry (BT) reward model (90% weight) and a lightweight format-based reward (10% weight). The BT reward<sup>7</sup> evaluates the quality of user summaries in the `<thinking>` section based on contrastive training with expert samples (See Section A.3). The format-based reward ensures syntactic correctness of ranked outputs (e.g., `<ranking>[800691007], [800691016], [752512008]</ranking>`).

This combined reward forms the sequence-level terminal reward  $r^{(g)}$  in Algorithm 1. When applying PBRS (Ng et al., 1999) normalization at the token level (Step 16), the efficiency property ( $\sum_{t=1}^T \phi_t = r^{(g)}$ ) ensures the sum of token-level attributions equals the total reward. Since PBRS simply scales attributions to match the sequence reward, using a weighted combination of rewards preserves the theoretical guarantees of Owen-value attribution while providing practical training benefits.

**Candidate Pool Construction** To stabilize RL training during product search tasks, we sample query-specific candidate pools that densify reward signals and are shared across GRPO and OSPO for fairness. During evaluation, the same filtered setting is used for consistency. For **ESCI**, we use the US Exact-Match subset, keeping queries with 3–10 relevant products. Direct NDCG over top-1000 FAISS results proved too sparse, so we build 100-item pools per query containing ground-truths, hard negatives (same category), related-category distractors, and random items. This yields denser, more informative rewards. For **H&M**, each query has one ground-truth target; we form analogous 100-item pools with that target plus 99 negatives sampled from similar categories.

**Hyperparameters** All RL training runs use **Qwen2.5-7B-Instruct** with learning rate 5e–6, batch size 8, and gradient accumulation over 2 steps for 2000 updates. Maximum prompt/completion lengths are 256/356 tokens for ESCI, 356/512 for H&M, and 900/800 for user summarization. These settings are shared across OSPO and GRPO. Following (Lin et al., 2025), we set  $\beta=0.0$  for KL regularization and use FAISS with top- $k=1000$  retrieval for reward computation. We

<sup>7</sup>BT scores are normalized to  $[0, 1]$  using stable min–max normalization  $(r - r_{\min}) / (r_{\max} - r_{\min})$ , with empirical global bounds  $r_{\min} = -5$  and  $r_{\max} = 10$  estimated over the dataset.

**System Prompt:** You are a query refinement specialist. Your task is to transform customer queries into product-focused descriptions while retaining all essential information from the original query.

**Write your analysis in `<think>` tags by first identifying the customer’s core need**, then noting the specific attributes they mentioned (fit, color, style, occasion, material), and finally checking if purchase history reveals relevant patterns.

Then **output your refined query in `<answer>` tags as 2–3 natural sentences** written as a product description. Start directly with product features. Focus on materials, style, and how it addresses the need. **Do not** start with phrases like “The customer needs” or invent details not present in the query or purchase history. Add coordination with purchase history items only when a clear pattern exists.

**User Input:**

<INPUT QUERY> (I need a new black top, maybe something with embroidery or smocking. Not too tight or low-cut, I prefer a relaxed fit.)

**Purchase History:**

```

Pirat leggings -- Leggings/Tights in Black
DIV Swift jumper -- Sweater in Dark Blue
CHERRY JRSY SKIRT -- Skirt in Black
Control Lt 40 den 2p Tights -- Underwear Tights in Black
Jiminy -- Sweater in Off White
Bono NW slim denim -- Trousers in Light Blue
Wille boot -- Boots in Black
Bono NW slim denim -- Trousers in Dark Grey
Luna skinny 5 pkt -- Trousers in Light Pink
Skirt Pencil Stretch Slit -- Skirt in Black

```

*Figure 5.* Full prompt used for training and evaluation on the H&M Fashion dataset. Unlike ESCI, this setup grounds the LLM’s instructions in the user’s *purchase history* for contextualized query refinement. Only the text within `<answer>` tags is used for Owen value computations in OSPO, while the `<think>` section supports intermediate CoT reasoning. The example query shown in purple is drawn from the dataset.

additionally filter the FAISS-retrieved top-k items based on a candidate pools of relevant items, collected prior to training in each domain. Each prompt samples 8 generations for stable advantage estimates. For OSPO, coalition width  $w_{\max}=8$  and 64 permutations per sequence balance local context and diversity; only *contiguous* coalitions are used for semantically coherent Owen value assignments (Algorithm 1).

## A.5. Additional Results

**Generalization Under Retriever Shift.** Table 4 and Table 1 together evaluate the *cross-retriever robustness* of alignment methods—how well trained policies maintain ranking quality when tested with a different embedding and retrieval backbone. Specifically, GRPO and OSPO were trained on ESCI using ALL-MPNET-BASE-V2 embeddings and FAISS indices, and are re-evaluated with SIMCSE-LARGE; the reverse is applied to the H&M domain. *his bi-directional setup tests how policies generalize when exposed to new embedding geometries and reward spaces unseen during training.*

As shown in Table 4, **OSPO-PROP** demonstrates strong generalization on ESCI product search, substantially outperforming all baselines across NDCG, MRR, and AP, confirming its ability to preserve task-specific robustness and quality with fine-grained credit assignment even under embedding shifts. In the H&M product search task, OSPO additionally maintains consistent gains over GRPO, though the absolute values are lower due to cross-domain retriever mismatch. The “offline” baselines (DPO, SFT) perform moderately well in-domain but degrade sharply under retriever shift, underscoring their reliance on static supervision without retrieval-grounded feedback. Similarly, larger Qwen models (14B, 72B) show limited transfer, reinforcing that scale alone does not ensure robustness across retrieval domains.

When comparing against the in-domain results from Table 1, we observe the expected performance drop under cross-retriever evaluation. For example, **OSPO-PROP** in H&M—drops from NDCG = 0.436 and Recall = 0.486 to 0.190 and 0.240 respectively, while GRPO declines from 0.380 to 0.184. Despite this degradation, OSPO variants consistently retain higher relative performance and more stable recall than GRPO, illustrating its improved generalization and robustness to embedding-space and reward-model variations. In the ESCI domain product search, the same pattern holds: all methods experience performance loss when tested with the alternate retriever, but **OSPO-PROP remains the strongest overall**, surpassing both reinforcement and supervised baselines even under out-of-distribution (OOD) retriever settings.

Baseline	ESCI				H&M			
	NDCG	AP	MRR	Recall	NDCG	AP	MRR	Recall
SFT (7B)	0.1761	0.1158	0.4004	0.1166	—	—	—	—
DPO (7B)	0.2280	0.1325	0.4412	0.1330	—	—	—	—
GRPO	0.2257	0.1144	0.3887	0.1150	0.1844	0.1681	0.1681	0.2348
Qwen2.5-0.5B	0.2183	0.1121	0.3757	0.1127	0.1453	0.1323	0.1323	0.1851
Qwen2.5-1.5B	0.2926	0.1382	0.4648	0.1390	0.2158	0.1986	0.1986	0.2687
Qwen2.5-3B	0.2109	0.1209	0.4128	0.1217	0.1504	0.1392	0.1392	0.1851
Qwen2.5-14B	0.2628	0.1583	0.5202	0.1592	—	—	—	—
Qwen2.5-32B	0.2549	0.1581	0.5135	0.1597	0.2025	0.1836	0.1836	0.2607
Qwen2.5-72B	<b>0.2986</b>	<b>0.1748</b>	<b>0.5766</b>	<b>0.1759</b>	0.1621	0.1446	0.1446	0.2159
<b>OSPO (Prop) (ours)</b>	<b>0.3691</b>	<b>0.1673</b>	<b>0.5395</b>	<b>0.1683</b>	<b>0.1901</b>	<b>0.1739</b>	<b>0.1739</b>	<b>0.2398</b>
<b>OSPO (Rank) (ours)</b>	0.2675	0.1468	0.4888	0.1475	0.2019	0.1846	0.1846	0.2557

**Table 4. Cross-Retriever Evaluation on Product Search Tasks.** RL baselines GRPO and OSPO were trained on the ESCI domain using dense retrieval rewards computed with ALL-MPNET-BASE-V2 embeddings and a FAISS HNSW index for similarity search. For evaluation, we test generalization under a retriever shift by re-encoding sampled refined queries in both ESCI and H&M evaluation input queries using SIMCSE-LARGE. This setting measures *cross-retriever robustness*—how well alignment methods such as OSPO and GRPO preserve ranking quality when the embedding space and retrieval backbone differ from those used during training.

## A.6. Coalition Formation and Sampling Strategy

Our approach to computing Owen-Shapley (Owen, 1977; 2014) attributions requires evaluating the marginal contribution of each segment across multiple coalitions. We now detail how we construct these coalitions and manage the computational trade-offs inherent in this process.

**Contiguous Coalition Generation.** Given a response  $y^{(g)}$  sampled from the policy  $\pi_\theta$  during OSPO training, we decompose it into  $N$  segments  $\mathcal{A}^{(g)} = \{a_1, \dots, a_N\}$  via linguistic phrase extraction for product search tasks (where segments are clauses) or regex-based sentence splitting for user summary generation tasks. We then generate contiguous coalitions—subsets of consecutive segments that preserve the sequential structure of the response. Formally, a coalition  $S$  is *contiguous* if  $S = \{i, i+1, \dots, i+w-1\}$  for some starting position  $i \in \{1, \dots, N\}$  and width  $w \in \{1, \dots, \min(w_{\max}, N)\}$ . This contiguity constraint ensures that coalition-based partial segments  $y_S$  remain semantically coherent—a critical requirement for meaningful reward evaluation in our tasks.

The complete set of contiguous coalitions  $\mathcal{C}$  includes:

- The **empty coalition**  $\emptyset$ , representing no query (baseline reward<sup>8</sup> of 0)
- All **contiguous windows** of width  $w = 1, \dots, \min(w_{\max}, N)$
- The **full coalition**  $\{1, \dots, N\}$ , representing the complete response

The total number of possible contiguous coalitions is:

$$|\mathcal{C}| = 1 + \sum_{w=1}^{\min(w_{\max}, N)} (N - w + 1) \quad (24)$$

where the summation counts all starting positions for each width  $w$ , and the leading 1 accounts for the empty coalition. For example, with  $N = 5$  segments and  $w_{\max} = 3$ :

- Width 1:  $\{1\}, \{2\}, \{3\}, \{4\}, \{5\}$  (5 coalitions)
- Width 2:  $\{1, 2\}, \{2, 3\}, \{3, 4\}, \{4, 5\}$  (4 coalitions)

<sup>8</sup>In practice, for the user summary generation task—where the reward function  $r(x, y_{S_m})$  depends on the context  $x$ —we allow for negative baseline rewards. Note that rewards for search tasks that are assigned by a retriever acting as a reward model only depend on the partial query  $y_{S_m}$  and not on the context.

- Width 3:  $\{1, 2, 3\}, \{2, 3, 4\}, \{3, 4, 5\}$  (3 coalitions)

yielding  $|\mathcal{C}| = 1 + 5 + 4 + 3 = 13$  total coalitions including the empty and full coalitions.

**Computational Budget and Sampling.** Computing rewards for all coalitions becomes expensive and computationally intractable as  $N$  grows, since  $|\mathcal{C}| = O(N \cdot \min(w_{\max}, N))$ . To maintain tractability, we impose a sampling budget  $M$  (see Algorithm 1) that caps the number of coalitions evaluated per response. The actual number of sampled coalitions is:

$$k = \min(M, |\mathcal{C}|) \quad (25)$$

When  $|\mathcal{C}| \leq M$ , we evaluate all possible coalitions, providing exact Owen-Shapley values. When  $|\mathcal{C}| > M$ , we sample  $M$  coalitions using the following strategy:

- Anchor coalitions:** Always retain  $\emptyset$  and  $\{1, \dots, N\}$ , as these provide essential boundary conditions for marginal contribution estimates
- Random sampling:** Uniformly sample  $M - 2$  coalitions from the remaining  $|\mathcal{C}| - 2$  candidates

This sampling strategy ensures that our Owen value estimates remain well-calibrated: the empty coalition anchors the baseline, while the full coalition captures the terminal reward. The intermediate coalitions provide estimates of each segment's contribution across diverse contexts.

**Coalition Evaluation.** For each sampled coalition  $S_m \in \{S_1, \dots, S_k\}$ , we construct the partial query  $y_{S_m}$  by concatenating the corresponding segments in order:

$$y_{S_m} = a_i \oplus a_{i+1} \oplus \dots \oplus a_{i+w-1} \quad \text{where } S_m = \{i, i+1, \dots, i+w-1\} \quad (26)$$

and evaluate its coalition value  $v(S_m) = r(x, y_{S_m})$  using our reward function. In our search task, this involves issuing  $y_{S_m}$  as a query to the retrieval system and computing the NDCG@1000 score against the target item(s). The empty coalition receives  $v(\emptyset) = 0$  by convention, reflecting the absence of information.

**Contiguity Rationale.** Our choice to restrict coalitions to contiguous subsets—rather than exploring all  $2^N$  possible subsets—is motivated by both computational efficiency and semantic coherence. Non-contiguous coalitions (e.g.,  $\{1, 3, 5\}$  skipping segments 2 and 4) would produce fragmented queries that (a) require  $O(2^N)$  evaluations, and (b) may yield semantically incoherent text, confounding reward evaluation and possibly lead to performance degradation due to the loss of local structure and high-variance Owen value estimates. Contiguity preserves the narrative flow of the response while reducing complexity to  $O(N \cdot w_{\max})$ , making Owen value estimation tractable for online RL training. In fact, our ablation study on coalition sampling in Section A.7 suggests that non-contiguity in sampling can lead to a significant performance drop in conventional product search task on ESCI dataset.

**Illustrative Example.** Consider a response  $y^{(g)}$  with extracted phrases:

$$\begin{aligned} a_1 &= \text{“blue midi dress”} \\ a_2 &= \text{“summer wedding”} \\ a_3 &= \text{“elegant style”} \end{aligned}$$

With  $w_{\max} = 4$  and  $M = 32$ , we generate  $|\mathcal{C}| = 1 + 3 + 2 + 1 = 7$  coalitions:

Coalition $S_m$	Partial Query $y_{S_m}$
$\emptyset$	(empty, $v(\emptyset) = 0$ )
$\{1\}$	“blue midi dress”
$\{2\}$	“summer wedding”
$\{3\}$	“elegant style”
$\{1, 2\}$	“blue midi dress summer wedding”
$\{2, 3\}$	“summer wedding elegant style”
$\{1, 2, 3\}$	“blue midi dress summer wedding elegant style”

Ablation	NDCG	Recall	MRR	AP
<b>num_generations = 8</b>				
OSPO-w8-p96	0.7821	0.8375	0.7625	0.7625
OSPO-w16-p256	0.7637	0.8375	0.7375	0.7375
OSPO-w2-p64	0.7558	0.8250	0.7312	0.7312
OSPO-w3-p24	0.7545	0.8375	0.7250	0.7250
OSPO-w6-p32	0.7525	0.8125	0.7312	0.7312
OSPO-w1-p16	0.7183	0.7875	0.6937	0.6937
OSPO-w4-p48	0.7058	0.7750	0.6813	0.6813
OSPO-w12-p128	0.5946	0.6500	0.5750	0.5750
<b>num_generations = 2</b>				
OSPO-w8-p96	0.2500	0.2500	0.2500	0.2500
OSPO-w2-p64	0.2375	0.2375	0.2375	0.2375
OSPO-w1-p16	0.2375	0.2375	0.2375	0.2375
OSPO-w12-p128	0.2250	0.2250	0.2250	0.2250
<b>All Subsets</b>				
OSPO-w4-p8	0.1625	0.1625	0.1625	0.1625
OSPO-w4-p16	0.1329	0.1375	0.1313	0.1313
OSPO-w8-p16	0.1125	0.1125	0.1125	0.1125
OSPO-w8-p8	0.0408	0.0500	0.0375	0.0375

Table 5. Ablation results on the ESCI product search benchmark for OSPO-PROP variants. Each entry reports the mean performance across 10 evaluations (every 100 steps of training) conducted on 100 randomly sampled queries from the ESCI evaluation set. Here, **w** denotes the maximum coalition span ( $w_{max}$ ) and **p** the number of coalitions sampled ( $M$ ) for Owen value estimation in OSPO (Algorithm 1).

Since  $|\mathcal{C}| = 7 < M = 32$ , all coalitions are evaluated. Each query is submitted to the search system, producing coalition values  $\{v(S_m)\}_{m=1}^7$ . For instance, if the target item is a blue dress suitable for weddings, we might observe  $v(\{1\}) = 0.6$ ,  $v(\{1, 2\}) = 0.85$ , and  $v(\{1, 2, 3\}) = 0.82$ . The marginal contribution of segment  $a_2$  in the context of  $S = \{1\}$  is then  $v(\{1, 2\}) - v(\{1\}) = 0.25$ , quantifying how “summer wedding” refines the query when added to “blue midi dress.” These marginal contributions across all applicable coalitions are aggregated via the Owen-Shapley formula to produce the final attribution  $\phi_2$  for segment  $a_2$ .

#### A.7. Ablations Study on Coalition Formation

In order to identify the most effective coalition configuration for OSPO optimization, we conduct a series of experiments across multiple coalition settings to guide hyperparameter selection. To analyze the role of coalition structure more precisely, we perform additional ablations on both product search tasks by systematically varying two key parameters that govern Owen value estimation in OSPO as mentioned in Section A.6. Specifically, **w** denotes the maximum coalition span ( $w_{max}$ ), which determines the widest contiguous segments that can be included in a coalition, while **p** denotes the number of coalitions sampled ( $M$ ) for estimating the expected marginal contribution of each token (via segments) under the Owen value framework (Algorithm 1). We additionally include an **All Subsets** variant that removes the contiguity constraint (Line 5 in Algorithm 1) by sampling from “all” possible non-contiguous coalitions up to  $w_{max}$ , allowing us to assess how the loss of local structure and linguistic contiguity affect marginal contribution estimation.

**Coalition Structure and Exploration as Drivers of Stable and Generalizable Learning.** As summarized in Table 5, OSPO’s performance in the conventional product search task on ESCI shopping queries is governed by the interaction between *coalition structure* and *exploration*. Moderate, contiguous configurations (e.g., w8-p96, w6-p32) consistently yield the strongest NDCG/MRR—balancing local compositional context with sufficient permutation diversity—whereas very narrow coalitions (e.g., w1, w2) overfit to local co-occurrences, and very wide coalitions (e.g., w12, w16) underutilize the sampling budget given typical query lengths. All Subsets variants underperform because they discard contiguity and disperse a fixed sampling budget over an exponentially larger non-contiguous space, producing high-variance Owen estimates and a weaker token-level credit signal. Reducing Monte Carlo generations further degrades scores across the board, underscoring that exploration via REINFORCE-based (Williams, 1992b; Shao et al., 2024a) multiple completions is indispensable for stable advantage redistribution in OSPO. These trends mirror our H&M fashion results for contextualized product search task—best generalization arises from *contiguous, moderate-width coalitions with adequate permutations and generation sampling*, rather than from either extremely narrow/wide spans or non-contiguous subset sampling.

Method	Final NDCG	Mean NDCG	Std NDCG	Max NDCG
w4_p48	0.625000	0.688851	0.114355	0.972842
w3_p24	0.609375	0.689658	0.113945	0.968750
w16_p256	0.593750	0.688587	0.111952	1.000000
w2_p64	0.587983	0.687731	0.109890	0.953125
w12_p128	0.578125	0.686309	0.111869	0.968750
w8_p96	0.562500	0.687286	0.111027	0.953125
w6_p32	0.562500	0.686912	0.112748	0.962983
w1_p16	0.546875	0.691219	0.110675	0.957217

Table 6. Training performance (NDCG) on the H&M contextualized product search dataset. Values reported at the final checkpoint **step = 1000**; we also include mean, standard deviation, and maximum NDCG observed over training. Higher is better.

## A.8. Coalition Width and Learning Dynamics

Our ablation reveals a non-monotonic relationship between coalition width and generalization performance, with distinct learning dynamics emerging across the spectrum.

### A.8.1. SMALL COALITIONS: FAST LEARNING, EARLY COLLAPSE

Narrow coalition widths (w2\_p64) exhibit rapid initial learning, achieving NDCG 0.75 by step 200, but subsequently degrade catastrophically to 0.44 by step 1000. This pattern reflects a fundamental trade-off: smaller coalitions converge quickly by identifying surface-level patterns (e.g., “black jeans” or “high waist” as isolated features), but lack the compositional structure needed to capture how multiple preference attributes interact.

The degradation after step 600 suggests that width-2 coalitions introduce noise into the credit assignment signal. When evaluating coalitions containing only 1–2 consecutive phrases, marginal contribution estimates become unstable—a single phrase’s Owen value fluctuates depending on which adjacent phrase appears in the coalition, without sufficient context to disambiguate genuine causal effects from spurious correlations. This instability causes the model to oscillate between competing hypotheses about which tokens drive performance, ultimately converging to a suboptimal solution that fails to generalize.

### A.8.2. VERY WIDE COALITIONS: UNDERUTILIZATION DUE TO QUERY LENGTH

Configurations with maximum width (w16\_p256) fail to outperform more moderate settings despite their theoretical expressiveness. Analysis of generated queries during training reveals the constraint: **most queries contain only 6–10 segmented phrases**, making width-16 coalitions impossible to construct. Even when the maximum permutation limit is set to 256, we observe that only approximately 41–48 unique coalitions are actually sampled per query, as the contiguous constraint combined with limited phrase count restricts the coalition space.

This underutilization has two consequences. First, the model cannot leverage the fine-grained credit assignment that wider coalitions theoretically enable—there simply aren’t enough phrases to form them. Second, the high permutation budget (256) is wasted on resampling similar small coalitions, rather than exploring diverse coalition structures. As a result, w16\_p256 performs no better than more efficient configurations with moderate widths, demonstrating that coalition strategy must account for the *actual* query structure distribution, not just the maximum possible width.

### A.8.3. MODERATE-WIDE COALITIONS: DELAYED BUT STABLE CONVERGENCE

The w12\_p128 configuration demonstrates a distinct learning profile: slower initial learning compared to small coalitions, but convergence to a stable solution with sustained performance. This configuration peaks around step 700 (NDCG 0.71) and maintains reasonable performance through step 1000, suggesting that width-12 coalitions provide sufficient compositional range for the task without exceeding typical query lengths.

However, w12\_p128 exhibits late-training instability (declining from 0.71 to 0.55 between steps 700–1000), indicating potential overfitting to the coalition structure itself. With 128 sampled coalitions per query, the model may learn spurious correlations specific to the training coalition distribution rather than robust compositional patterns.

#### A.8.4. OPTIMAL RANGE: W4\_P48 AS THE GOLDILOCKS CONFIGURATION

The configuration with width  $W = 4$  and  $P = 48$  permutations achieves the best final performance (NDCG 0.71) through a qualitatively different learning trajectory. Unlike narrow coalitions that peak early or wide coalitions that show volatility, w4\_p48 exhibits **gradual, monotonic improvement** throughout training, with its steepest gains occurring in the final 400 steps (0.63 at step 600  $\rightarrow$  0.71 at step 1000).

This delayed convergence reflects a more principled learning process. Width-4 coalitions can capture meaningful multi-attribute patterns (e.g., “black skinny jeans + stiff fabric”) without requiring query lengths that rarely occur. The moderate permutation count (48) provides sufficient diversity for robust Owen value estimation without oversampling, avoiding both the noise of w2\_p64 and the overfitting risk of w12\_p128.

Critically, w4\_p48’s continued improvement in late training—when other configurations plateau or degrade—suggests it has not converged to a local optimum exploiting training-specific patterns. Instead, the gradual ascent indicates the model is progressively refining its understanding of compositional query semantics, leading to solutions that generalize to novel test cases.

#### A.8.5. THE ROLE OF COALITION NOISE

The dramatic failure of w2\_p64 (collapsing from 0.75 to 0.44) and instability of w1\_p16 validate a key intuition: **coalition width acts as a regularization parameter**. Excessively narrow coalitions introduce noise by providing insufficient context for stable marginal contribution estimates. When Owen values are computed from coalitions containing only 1–2 tokens, the credit signal becomes dominated by local interactions rather than compositional semantics.

This noise has a delayed effect—early training benefits from rapid exploitation of surface patterns, but as training progresses, the accumulation of noisy credit assignments leads the model to overweight spurious features. By contrast, width-4 coalitions filter this noise by requiring evaluation contexts large enough to disambiguate genuine compositional effects from random co-occurrences, leading to more stable and generalizable learning.

### A.9. Design Implications

These findings establish coalition width as a *critical hyperparameter* for OSPO, with optimal values determined by task-specific query structure:

- **Task constraint:** Coalition width must match typical query complexity. For product search with 6–10 segmented phrases,  $W \in \{4, 6, 8\}$  provides the sweet spot.
- **Noise-stability trade-off:** Widths  $< 3$  introduce excessive noise; widths  $> 12$  waste capacity on unattainable coalitions.
- **Convergence profile:** Moderate widths (w4) show delayed but stable learning, while extremes (w2, w16) either collapse or plateau prematurely.
- **Permutation budget:** Should scale with achievable coalition diversity, not just theoretical maximum. For width-4 with 8 phrases,  $P = 48$  suffices;  $P = 256$  provides no additional benefit.

The non-monotonic relationship between coalition width and performance—where both too-narrow and too-wide configurations underperform—demonstrates that fine-grained credit assignment in OSPO requires careful calibration to the task’s semantic structure.

**Ablation on Coalition Width and Sampling Count.** We analyze the effect of coalition configuration parameters on OSPO-PROP training performance in contextualized product search task in the H&M Fashion domain, focusing on the maximum coalition width ( $w$ ) and the number of sampled coalitions ( $p$ ) used in Owen value estimation. Results are summarized in Table 7. Due to compute constraints, we down-sample the contextualized search training data to 1,000 samples and evaluate on 100 held-out samples after one training epoch. To cover a broad configuration space efficiently, we use the Qwen 2.5–1.5B–Instruct model for this ablation.

**Coalition width ( $w$ ).** As shown in Table 7, moderate widths ( $w=4–6$ ) yield the highest ranking quality (NDCG  $\approx 0.36$ ), while both narrow ( $w \leq 2$ ) and wide ( $w \geq 12$ ) configurations underperform (NDCG  $\leq 0.33$ ). This reflects a trade-off between

Configuration	Max Width	NDCG	Avg. Tokens	Zero Rate
w1_p16	1	0.222	145.6	43.8%
w2_p32	2	0.264	173.7	50.0%
w2_p64	2	0.332	165.9	12.5%
w3_p48	3	0.237	202.5	31.2%
w4_p24	4	<b>0.360</b>	191.7	<b>6.2%</b>
w6_p64	6	<b>0.360</b>	149.3	12.5%
w8_p96	8	0.300	199.1	40.6%
w12_p128	12	0.349	157.0	18.8%
w12_p256	12	0.271	132.1	43.8%

Table 7. Owen–Shapley coalition ablation results after one epoch, evaluated on the training set using 1,000 samples for efficiency. Experiments use the Qwen 2.5–1.5B–Instruct model. Here, **w** denotes the maximum coalition span (consecutive phrases) and **p** the number of coalitions sampled for Owen value estimation. In the OSPO algorithm (Algorithm 1), **w** corresponds to the maximum coalition width  $w_{\max}$  and **p** to the total number of sampled coalitions  $M$ . NDCG@1000 measures ranking quality on pooled retrieval candidates, and **Zero Rate** denotes the proportion of completions with zero reward. Best values are highlighted in bold.

contextual coverage and noise accumulation. Wider coalitions concatenate more extracted phrases, increasing the chance of mixing meaningful segments (e.g., “comfortable jeans”, “breathable linen”) with fragmentary artifacts (e.g., “- wash”, “a step”). This arises from the spaCy<sup>9</sup> phrase extraction pipeline, which can occasionally capture short or incomplete fragments when forming noun or verb-led spans. When such noisy fragments are concatenated under large coalition widths, they distort semantic coherence and yield incoherent queries (e.g., “comfortable jeans a weekend outing - wash mid wash”). As a result, Owen–Shapley credit assignment distributes marginal contributions across irrelevant tokens, weakening policy updates. Moderate-width coalitions, by contrast, preserve compositional context while suppressing spurious phrase interactions, producing clearer and more focused learning signals.

**Coalition sampling count ( $p$ ).** The number of sampled coalitions controls the variance of the Owen value approximation. Moderate sampling densities ( $p=24\text{--}64$ ) implicitly regularize training by limiting exposure to noisy phrase combinations, yielding both high NDCG and low zero-reward rates (6–12%). Excessively large  $p$  values ( $p=256$ ) degrade ranking quality (NDCG 0.27) and increase the fraction of zero-reward samples (43.8%), as exhaustive coalition coverage overfits to irrelevant phrase subsets and disperses credit too broadly. This indicates that stochastic coalition sampling not only reduces computational cost but also stabilizes the reward signal during policy optimization.

**Assessing reward hacking.** To investigate whether OSPO-PROP exhibits reward hacking through query length manipulation, we compute the Pearson correlation coefficient between query length (in tokens) and reward across all configurations in Table 7. The observed correlation of  $-0.165$  indicates a weak negative relationship, meaning longer queries tend to perform slightly *worse* rather than better. This finding provides little evidence of reward hacking—if models were exploiting length to maximize rewards (Skalse et al., 2025), we would observe a strong positive correlation instead. The weakness of this correlation (close to zero) further suggests that query length is not a primary driver of retrieval performance; rather, semantic coherence and phrase quality matter more for effective search query generation under OSPO-PROP.

**Coalition Reward Patterns.** To understand how coalition composition affects retrieval performance, we examine individual coalition-level rewards during training. Successful coalitions (non-zero rewards) consistently combine three key elements: concrete product identifiers (e.g., jeans”, coat”, dress”), specific attributes (e.g., mid-blue wash”, high-waist”, ankle length”), and customer intent or use-case context (e.g., weekend outing”, beach vacation”). For example, the coalition *your current wardrobe various situations cooler spring days a rich blue hue shorter length neutral colors a coat*” achieves perfect reward (1.0) by balancing contextual framing with discriminative product features. In contrast, coalitions receiving zero reward fall into predictable failure modes: generic phrases without product anchors (a pair”, modern fit”), pure adjective sequences lacking concrete nouns (sleek polished clean”), junk phrase contamination from parsing artifacts (- wash”, a step”), or excessive repetition and incomplete fragments (few lightweight... lightweight... a touch”). Notably, even coalitions containing strong individual phrases fail when dominated by vague descriptors; for instance, *prefer a vibrant color to add my usual neutral tones my beach vacation some personality*” receives zero reward despite capturing user preferences, because it lacks a specific product type or actionable attributes. This analysis suggests that moderate coalition widths (( $w=4\text{--}6$ )) succeed by maintaining sufficient phrase diversity to construct discriminative queries while avoiding the accumulation of noisy fragments that degrade semantic coherence in wider configurations.

<sup>9</sup><https://spacy.io/models/en>

**Prompt and Completion**

**System:** You are a personal fashion advisor and stylist. Analyze the shopping history and rank **all provided candidate items** from most to least recommended for the next purchase. Consider style evolution, wardrobe needs, and purchasing patterns. Respond using `<thinking> [analysis] </thinking>` and `<ranking> [ordered item IDs] </ranking>`.

**User:** 25 years old, inactive club member, no fashion news subscription.

**Purchase history (summarized):** sweaters, leggings, bodysuits, trousers, and tops (2018–2019), primarily in pastel or neutral tones and low price range (\$0.01–\$0.02).

**Candidate items:** a mix of garments including swimsuits, a garment set, bodysuits, caps, bikini tops, trousers, blazers, dresses, and tops. Example entries include:

1. [742933003]: C Jackpot Swimsuit – Swimsuit in Black (\$0.03)
2. [767228001]: FASHION OFFER GRAYHAM SET – Garment Set in Off White (\$0.02)
3. [630416003]: Timber L/S Body – Bodysuit in Red (\$0.01)

...

9. [895993004]: Dag Tank – Vest top in Light Beige (\$0.01)

10. [822180002]: Tula – Sweater in Black (\$0.03)

**Assistant:**

`<thinking>`

Analyzing the customer's purchase history, it's clear that they have strong preferences for comfortable, modest-priced items and that they frequently purchase basic pieces like sweaters, undergarments, and simple tops. Each purchase has been around the \$0.01 mark, indicating a budget-conscious shopper. They have also purchased a variety of colors with an emphasis on pastels and neutral tones. Given their current inactivity and club member role, they might be looking for a more stylish yet comfortable piece that can be worn for various occasions, including social events.

Here's my analysis: The swimwear (item 1) and sporty top (item 5) are not suitable as purchases since there is no mention of beach trips or fitness activities. The blazer (item 7) is expensive and more formal, which does not align with their purchase history and budget. The high-end dress (item 8) would be a significant jump in price and might be out of their comfort zone, considering their current dresses were all within the \$0.01 price range. The expensive sweaters (items 10 and 3) are not suitable given their consistent purchase price. Items 2, 6, 9, and 4 (FASHION OFFER GRAYHAM SET, Lilja trousers, Dag Tank, and KELLY basic P-CAP) are all within the \$0.02–\$0.03 price range and offer different styles that fit well with their wardrobe. Considering the current fashion and the customer's budget and preferences, I recommend a versatile item with a neutral color and casual-chic look.

`<ranking> [767228001, 895993004, 790057001, 811907005] </ranking>`

Table 8. Table showing an illustrative user summary generated by the OSPO-PROP-trained Qwen2.5-7B-Instruct model in the user summary generation task (main results in Table 2). System and user prompts are trimmed for brevity.

Together, these findings suggest that **OSPO-PROP achieves optimal balance at moderate coalition configurations** ( $w=4\text{--}6$ ,  $p=24\text{--}64$ ), where the phrase context is sufficiently rich to capture meaningful dependencies but constrained enough to avoid semantic drift. The corresponding low zero-reward rates and stable token lengths further confirm that controlled coalition sampling preserves dense and informative gradients, leading to robust policy learning and higher downstream ranking quality.

S#	Sentence Text
S0	Analyzing the customer's purchase history, it's clear that they have strong preferences for comfortable, modest-priced items and that they frequently purchase basic pieces like sweaters, undergarments, and simple tops.
S1	Each purchase has been around the \$0.01 mark, indicating a budget-conscious shopper.
S2	They have also purchased a variety of colors with an emphasis on pastels and neutral tones.
S3	Given their current inactivity and club member role, they might be looking for a more stylish yet comfortable piece that can be worn for various occasions, including social events.
S4	Here's my analysis:
S5	The swimwear (item 1) and sporty top (item 5) are not suitable as purchases since there is no mention of beach trips or fitness activities.
S6	The blazer (item 7) is expensive and more formal, which does not align with their purchase history and budget.
S7	The high-end dress (item 8) would be a significant jump in price and might be out of their comfort zone, considering their current dresses were all within the \$0.01 price range.
S8	The expensive sweaters (items 10 and 3) are not suitable given their consistent purchase price.
S9	Items 2, 6, 9, and 4 (FASHION OFFER GRAYHAM SET, Lilja trousers, Dag Tank, and KELLY basic P-CAP) are all within the \$0.02–\$0.03 price range, and offer different styles that can fit well with their wardrobe.
S10	Considering the current fashion and the customer's budget and preferences, I would recommend a versatile item that can fit most scenarios, thus likely a piece with a more neutral color and a casual yet chic look.
S11	<ranking> [767228001, 895993004, 790057001, 811907005] </ranking>

Table 9. OSPO User summary generation sample: Sentence-level reasoning breakdown from assistant completion. Each sentence corresponds to  $S_i$  in the coalition analysis.

ID	Coalitions	Reward	Interpretation
0	[]	-3.2290	Empty user summary — baseline negative reward;
1	[0]	3.6821	First sentence alone carries strong global context (“preferences for comfortable, modest-priced items”). Establishes key signal.
2	[0,1]	4.4063	Early purchase-pattern reasoning (budget inference) compounds positively — synergy between S0 and S1.
3	[0,1,2]	4.7512	Adds color palette reasoning (S2), maintaining strong coherence; reward increases marginally.
4	[0,1,2,3]	3.4214	Adding lifestyle speculation (S3) introduces slight noise; reasoning starts to deviate.
5	[0,1,2,3,4]	4.7757	Meta-structure (“Here's my analysis:”) helps logical segmentation — reward briefly peaks.
6	[0–5]	-2.9897	Insertion of item-level exclusions (S5) sharply reduces relevance; excessive pruning or bias.
7	[0–6]	0.3499	Reintroduces structured filtering, partial recovery but still weak.
8	[0–7]	-1.0558	Over-constraint: adds formalwear exclusion (S7), possibly too harsh for general ranking.
9	[0–8]	-0.8890	Continues negative trend — overly restrictive logic misaligns with ground-truth ranking.
10	[0–9]	3.9120	Large recovery — includes specific candidate discussion (S9), capturing useful selection rationale. Highest observed reward before verbosity penalty.
11	[0–10]	3.0907	Adding generic stylistic recommendation (S10) slightly dilutes retrieval precision.
12	[0–11]	2.6979	End-of-trace expansion (ranking emission) inflates token count; diminishing returns.
13	[1–11]	1.8037	Excluding S0 removes global framing → coherence loss, partial reward drop.
14	[2–11]	2.1026	Partial recovery via descriptive attributes (S2), but weak without initial context.

Table 10. Coalition formation and rewards for sampled coalitions in the user profile summary generation task, where sentences act as “players” (segments). Each coalition’s reward is computed from sentence segments extracted from Chain-of-Thought traces of the Qwen2.5-7B-Instruct base model. The reward estimator is the same base model with a trained linear head on expert-generated contrastive user profile samples. Segment details are provided in Table 9.

## CONTEXTUALIZED QUERY GENERATION PROMPT

**User:** You are a customer behavior specialist. Generate realistic customer queries that reflect how people actually search for fashion items, based on their purchase history and personal shopping context

**Query Requirements:**

- Create five diverse queries (1–3 sentences each) targeting different candidate items.
- Vary types: explicit brand/style references, implicit descriptions, negations, underspecified needs.
- Include customer context: reference past purchases by name/style, seasonal timing, wardrobe gaps, price expectations.
- Use natural fashion language, not technical product descriptions.
- Include information gaps (missing colors, wrong categories, vague descriptions).

**Item Context Requirements:**

- Link customer needs to the specific product (why this item).
- Comparative references to owned items (e.g., “unlike my Julia denim trousers”).
- Underlying motivations (work confidence, wardrobe refresh, versatility, seasonal transition).
- Mix natural language *and* precise product terminology.
- State both what the customer wants *and* what they are avoiding.

**Example Query:**

“I need a black dress that’s more casual than my fitted Star knot velour dress but still looks put-together for spring. Something in that Tan dress style but in black since I’m tired of always wearing the same heavy pieces.”

**Example Item Context:**

“Spring-transition lightweight chiffon; casual-elegance alternative to heavy velour Star knot dress; work-to-weekend versatility; wrapover styling; breathable fabric; black foundation expands options; polished-casual aesthetic reduces outfit repetition.”

**Output Format:**

```
query1: <customer search query>
item_context1: <comprehensive matching description>
target_item_id1: <ITEM_ID>
[repeat for query2, query3, query4, query5]
```

Figure 6. Prompt used for H&M contextualized query generation using the Claude Sonnet 3 expert model

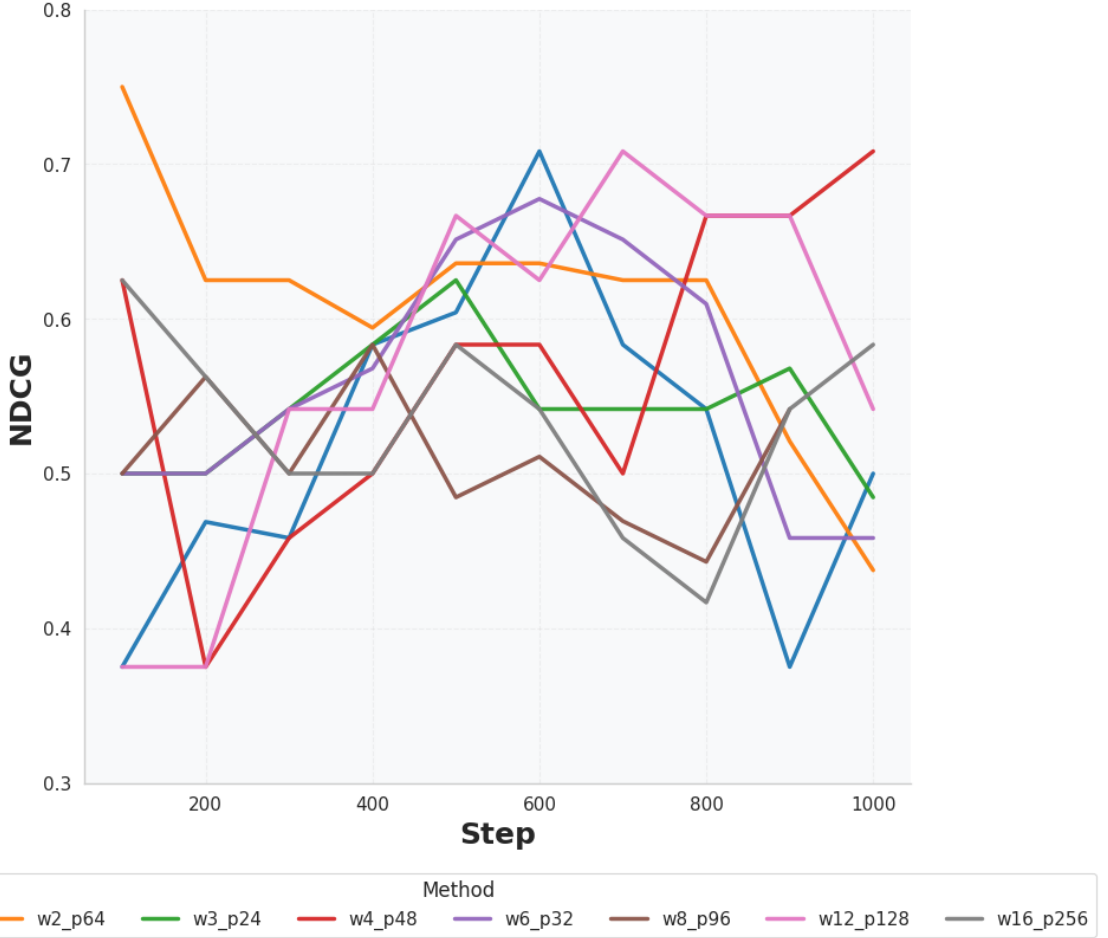


**Figure 7. Test NDCG on 100 H&M contextualized queries across coalition strategies.** We vary the **maximum span width**  $W \in \{1, 2, 3, 4, 6, 8, 12, 16\}$  and the **maximum permutation count**  $p \in \{16, 24, 32, 48, 64, 96, 128, 256\}$ . Medium-width configurations (e.g., w4\_p48, w6\_p32, w8\_p96) yield the most reliable evaluation trajectories and highest final NDCG (up to  $\approx 0.71$ ), while very small widths oscillate or degrade and large  $p$  values show diminishing returns given most contextualized queries are short with limited phrase diversity/domain-specificity. Here,  $w$  denotes the maximum coalition span ( $w_{max}$ ) and  $p$  the number of coalitions sampled ( $M$ ) for Owen value estimation in OSPO (Algorithm 1). These results indicate that coalition design mainly influences *generalization* rather than serving as a simple optimization hyperparameter.

Table 11. OSPO Rewards (Continued): Coalition combinations, rewards, and interpretive comments. Rewards correspond to partial-sentence subsets of the expert reasoning trace.

ID	Sentence Subset	Reward	Interpretation
15	[3–11]	1.8825	Retains lifestyle speculation but loses profile grounding; lower reward.
16	[4–11]	1.9275	Pure analysis section without framing; moderately neutral.
17	[5–11]	2.5463	Item-filtering logic dominates — fair local precision, low diversity.
18	[6–11]	2.5095	Similar to (17); mild degradation, redundant exclusions.
19	[7–11]	3.1307	Focus on mid/late reasoning; surprising bump — possibly due to item-specific reasoning (S9).
20	[8–11]	2.1938	Partial sentence window (S8–S11) lacks structure; reward decays.
21	[9–11]	2.9035	Captures shortlist discussion (S9–S11) — relevant but lacks justification context.
22	[10,11]	1.3301	Contains generic stylistic advice and ranking output; relevant but low semantic grounding.
23	[11]	0.5208	Ranking-only output; minimal information — weak semantic signal.
24	[1,2]	3.8981	Crucial early coalition: purchase habits + color reasoning; high consistency and relevance.
25	[2,3]	3.0590	Local coalition of color + lifestyle; moderate contextual fit.
26	[3,4]	3.8642	Transition from lifestyle to analysis marker — meaningful logical flow, strong local coherence.
27	[4,5]	0.0054	Weak handoff; introduction of filtering abruptly reduces clarity.
28	[5,6]	2.4154	Filtering criteria + pricing logic; regains some precision.
29	[6,7]	—	(Not logged) Likely small negative or neutral value given surrounding trend.
30	[7,8]	−0.4614	Consecutive exclusions (formal/dress) yield overfitting — retrieval misalignment.
31	[8,9]	0.0060	Weak positive recovery; transition toward item justification.
32	[9,10]	−0.7675	Adding stylistic advice to item shortlist confuses ranking criteria; drop in reward.